ADVANCED FUNCTIONAL MATERIALS
www.afm-journal.de

Integrating Engineered Living Materials with 3D Bioprinting

*Tae Seok Moon and Kyungsuk Yum**

Engineered living materials (ELMs) are an emerging class of biohybrid materials with genetically programmable functionalities. Integrating ELMs with 3D bioprinting synergizes their biological programmability with the geometry-driven functionality of 3D-printed constructs, transforming these materials into practical products and engineering solutions. This integration also introduces a new paradigm in additive manufacturing that harnesses the "livingness" of encapsulated microorganisms as an active element in the fabrication process to create adaptive and evolving 3D constructs. This Perspective presents recent advances in 3D bioprinting and discusses current developments at the intersection of 3D bioprinting and ELMs. It highlights opportunities at the interface of these two emerging fields, including understanding the interactions between living and nonliving components of ELMs for bioink design, incorporating synthetic biology into bioprinting workflows, utilizing microbial growth as a postprinting fabrication process, and integrating shape-morphing materials to enable the 4D printing of ELMs.

1. Introduction

Engineered living materials (ELMs) are an emerging class of materials that integrate living cells with nonliving matrices, creating biohybrid systems with programmable functionality.[1–6] The living cells are engineered with synthetic genetic circuits to perform user-defined tasks, while the nonliving matrices act as structural frameworks, providing a protective environment for the cells to grow and function. This synergy between living and nonliving components generates mechanically stable materials with adaptive and responsive functions similar to those of living organisms—features difficult or impossible to achieve with synthetic materials.

Synthetic biology enables the programming of cells within ELMs to execute diverse functions, such as sensing and responding to the environment, producing high-value compounds and materials, biocomputing, remediating harmful substances, and repairing material damage through self-healing.[7–10] These unique features unlock exciting opportunities for technological applications of ELMs, including wearable devices,[11,12] chemical and biological sensing,[13,14] living textiles and coatings,[15] material production,[16,17] bioremediation,[18–20] living building materials,[21,22] and biomedicine.[23–26] However, to realize the full potential of ELMs, a critical next step is to integrate them with manufacturing technologies that can process and transform them into mechanically robust constructs with desired geometries for intended applications.

3D bioprinting offers a promising platform for this integration. This technology builds 3D living constructs with customized geometries by depositing materials containing living cells, called bioinks or bioresins, layer by layer while maintaining cell viability.[27–34] The integration of 3D bioprinting and ELMs can merge the geometry-driven functionality of 3D-printed structures with the genetic programmability of ELMs, transforming these materials into practical products and engineering systems.

Traditional 3D bioprinting typically produces static constructs that support the viability of encapsulated cells and regulate their behavior within the constructs, primarily with one-way signal transfer from the printed materials to the cells. Beyond this capability, 3D bioprinting of ELMs enables dynamically evolving, adaptive constructs that leverage the "livingness" of the materials to grow, transform, reinforce, and repair printed materials. This feature fosters dynamic interplay between the printed materials and the encapsulated cells, enabling new capabilities for 3D printing. This bidirectional interaction can not only enhance the functionality of ELMs but also introduce a new paradigm for 3D printing that utilizes cellular processes in living materials as part of the fabrication process. This capability can enable the concept of "living" manufacturing, in which printed constructs grow toward predesigned forms or evolve in response to environmental stimuli.

Here, we present recent advances in 3D bioprinting and discuss current developments at the intersection of 3D bioprinting and ELMs. We provide our Perspective on future directions and opportunities at the interface of these two emerging technologies, highlighting key areas of interest. These include understanding the interactions between living and nonliving components of ELMs for bioink design, incorporating synthetic biology into bioprinting workflows, utilizing microbial growth as a postprinting fabrication process, and integrating shape-morphing

T. S. Moon
Synthetic Biology Group
J. Craig Venter Institute
La Jolla, CA 92037, USA
K. Yum
Department of Materials Science and Engineering
University of Texas at Arlington
Arlington, TX 76019, USA
E-mail: kyum@uta.edu

The ORCID identification number(s) for the author(s) of this article can be found under https://doi.org/10.1002/adfm.202500934

DOI: 10.1002/adfm.202500934

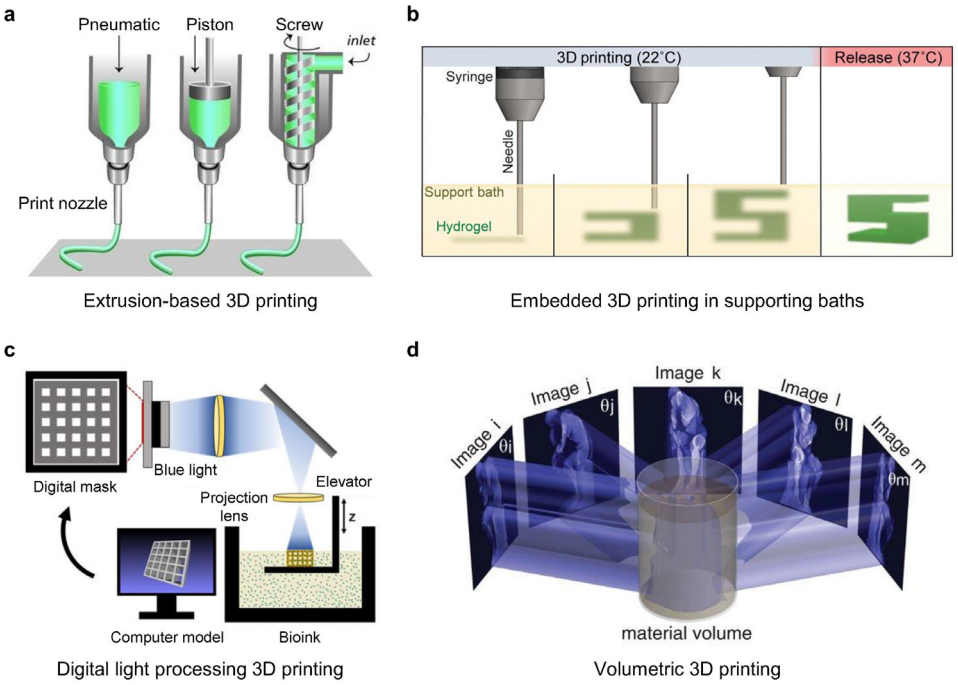

Figure 1. 3D Printing modalities for fabricating 3D structures of ELMs. a) Extrusion-based 3D printing. Reproduced with permission.[27] Copyright 2013, Wiley-VCH. b) Embedded 3D printing in supporting baths. Reproduced under terms of the CC-BY license.[55] Copyright 2015, The Authors, published by The American Association for the Advancement of Science. c) Digital light processing 3D printing. Reproduced under terms of the CC-BY-NC-ND license.[67] Copyright 2021, The Authors, published by American Chemical Society. d) Volumetric 3D printing. Reproduced with permission.[80] Copyright 2019, The American Association for the Advancement of Science.

materials with the 3D bioprinting of ELMs for their 4D printing. This Perspective focuses on ELMs composed of genetically engineered microorganisms, such as bacteria, fungi, and microalgae, embedded in hydrogel matrices. Accordingly, we emphasize the 3D bioprinting of ELMs using hydrogel-based bioinks, either hydrogel precursors or preformed hydrogels encapsulating engineered microbial cells. For a more comprehensive discussion on synthetic biology, genetically engineered microorganisms, and ELMs, we refer interested readers to other excellent reviews.[1–10]

2. 3D Bioprinting of Engineered Living Materials

3D bioprinting modalities that can be used to create 3D structures of ELMs include extrusion-based bioprinting, embedded bioprinting in support baths, light-based bioprinting, and volumetric bioprinting (**Figure 1**, **Table 1**).[27–34] Although initially developed to fabricate living tissues with mammalian cells, these techniques have been adapted to produce 3D constructs of ELMs (**Table 2**). Two essential components of 3D bioprinting are the

Table 1. Comparison of 3D bioprinting techniques.

	Extrusion-based printing	Embedded printing in support baths	Digital light processing printing	Volumetric printing
Printing process	Serial (layer by layer)	Serial (free form)	Parallel (layer by layer)	Volumetric
Printing speed	Slow (depends on structural complexity)	Slow (depends on structural complexity)	Fast (simultaneous crosslinking of an entire layer)	Very fast (simultaneous crosslinking of an entire 3D structure)
Printing resolution	Moderate (typically > 100 μm), limited by nozzle size and bioink rheology	Moderate to high (down to ≈10 μm)	High (down to ≈10 μm), defined by the precision of light projection and photocrosslinking	Moderate to high (down to ≈30 μm), influenced by optics and bioink transparency
Material compatibility	Extrudable bioinks	Broad range including low-viscous bioinks	Photocrosslinkable, low viscous bioinks	Transparent, photocrosslinkable bioinks
Advantages	Versatile, cost-effective, easy operation	Fabrication of complex structures, omnidirectional printing, extended printing time	High-throughput and high-resolution printing, fabrication of complex structures	Very fast printing, fabrication of complex, layer-free structures
Disadvantages	Slow printing (serial layer-by-layer process), limited resolution	Delicate extraction step, require support bath medium with well-controlled properties	Limited to photocrosslinkable bioinks	Limited to transparent, photocrosslinkable bioinks, require a large volume of bioink

Table 2. Representative studies on 3D bioprinting of ELMs.

Printing techniques	Bioinks		Postprinting crosslinking	Microbial cell functions	Refs.
	Microbial cells	Hydrogel matrices			
Extrusion-based bioprinting	*E. coli*	F127-DA	Photocrosslinking	Sensing AHL, IPTG, Rham, and aTc	[11]
	S. elongatus	Alginate	Ionic crosslinking	Laccase enzyme expression to decolorize a textile dye pollutant (indigo carmine), inducible cell death	[20]
	B. subtilis spores	Agarose	Physical crosslinking	Sense or kill *S. aureus*	[26]
	P. putida, *A. xylinum* (*G. xylinus*), *B. subtilis*	HA (or GMHA), κ-CA, and FS ("Flink")	Physical crosslinking (HA), photocrosslinking (GMHA)	Phenol degradation (*P. putida*), in situ formation of BC (*A. xylinum*)	[41]
	S. cerevisiae	F127-DMA	Photocrosslinking	Ethanol production using glucose	[45]
	S. cerevisiae (freeze-dried)	PEGDA and nanocellulose	Photocrosslinking	Ethanol production using glucose	[46]
	G. lucidum	Agar with κ-CA and cellulose-based thickener	Physical crosslinking	Self-repair, regeneration, self-cleaning	[47]
	E. coli	Alginate	Ionic crosslinking	Fluorescence	[48]
	B. subtilis	TasA amyloid fusion proteins with functional domains (amino acids)	Physical crosslinking	Secretion of TasA amyloid proteins with functional domains to degrade MHET and pesticide paraoxon	[49]
	E. coli	Curli nanofibers (CsgA-αβ; microbial ink)	Physical crosslinking	Release of an anticancer drug (azurin), sequestration of a toxic chemical (BPA), regulation of cell growth	[51]
	S. cerevisiae, *S.boulardii*	Acrylamide with CNC and BIS	Photocrosslinking	Proliferation in response to target amino acids (L-leucine, L-tryptophan, and L-histidine) and nucleotide (uracil)	[52]
Embedded bioprinting in support bath	*G. xylinus*	CNF Support bath material: PTFE microparticles	In situ biosynthesis of BC networks	In-situ biosynthesis of BC	[53]
	G. xylinus	Xanthan gum Support bath material: silicone microparticles and silicone	In situ biosynthesis of BC networks	In-situ biosynthesis of BC, self-healing through self-regeneration of BC	[54]
Digital light processing bioprinting	*E. coli*, *C. crescentus*	PEGDA	Photocrosslinking	Rare earth metal absorption and uranium sensing (*C. crescentus*)	[67]
	E. coli, *S. cerevisiae*	BSA conjugated with PEGDA	Photocrosslinking	Production of L-DOPA, naringenin, and betaxanthins	[68]
	S. cerevisiae	PEGDA	Photocrosslinking	Betaxanthin production	[69]

Microbial cells: *Ganoderma lucidum* (*G. lucidum*), *Saccharomyces boulardii* (*S. boulardii*), *Staphylococcus aureus* (*S. aureus*), *Synechococcus elongatus* (*S. elongatus*).Chemicals and materials: anhydrotetracycline (aTc), bisacrylamide (BIS), bisphenol A (BPA), cellulose nanocrystal (CNC), fumed silica (FS), glycidyl methacrylate hyaluronic acid (GMHA), isopropyl β-D-1-thiogalactopyranoside (IPTG), κ-carrageenan (κ-CA), MHET (mono(2-hydroxyethyl) terephthalic acid), *N*-acyl homoserine lactone (AHL), Pluronic F127-diacrylate (F127-DA), Pluronic F127-dimethacrylate (F127-DMA), rhamnose (Rham).

printing system and the bioink. Bioinks for ELMs primarily consist of microbial cells, such as bacteria, yeasts, and microalgae, and precursors for hydrogel matrices based on natural or synthetic polymers. An ideal 3D bioprinting platform would generate mechanically robust 3D constructs with high shape fidelity while providing a protective environment where microbial cells can thrive and function during and after printing. Additionally, due to the small size of microbial cells and their weak adhesion to hydrogel matrices, bioink design for ELMs needs to consider the physical containment of microbial cells to prevent unintended cell leakage from printed materials.[35–38]

2.1. Extrusion-based 3D Bioprinting

Extrusion-based 3D bioprinting is the most commonly used method for creating 3D living constructs (**Figure 2**).[33,34] This printing method builds 3D structures by extruding continuous filaments of bioinks through a print nozzle and depositing them into pre-designed geometries layer by layer (Figures 1a and 2). The printed structures are typically further stabilized through postprinting crosslinking, such as photocrosslinking, ionic crosslinking, and enzymatic crosslinking, which provides long-term structural stability and determines the mechanical

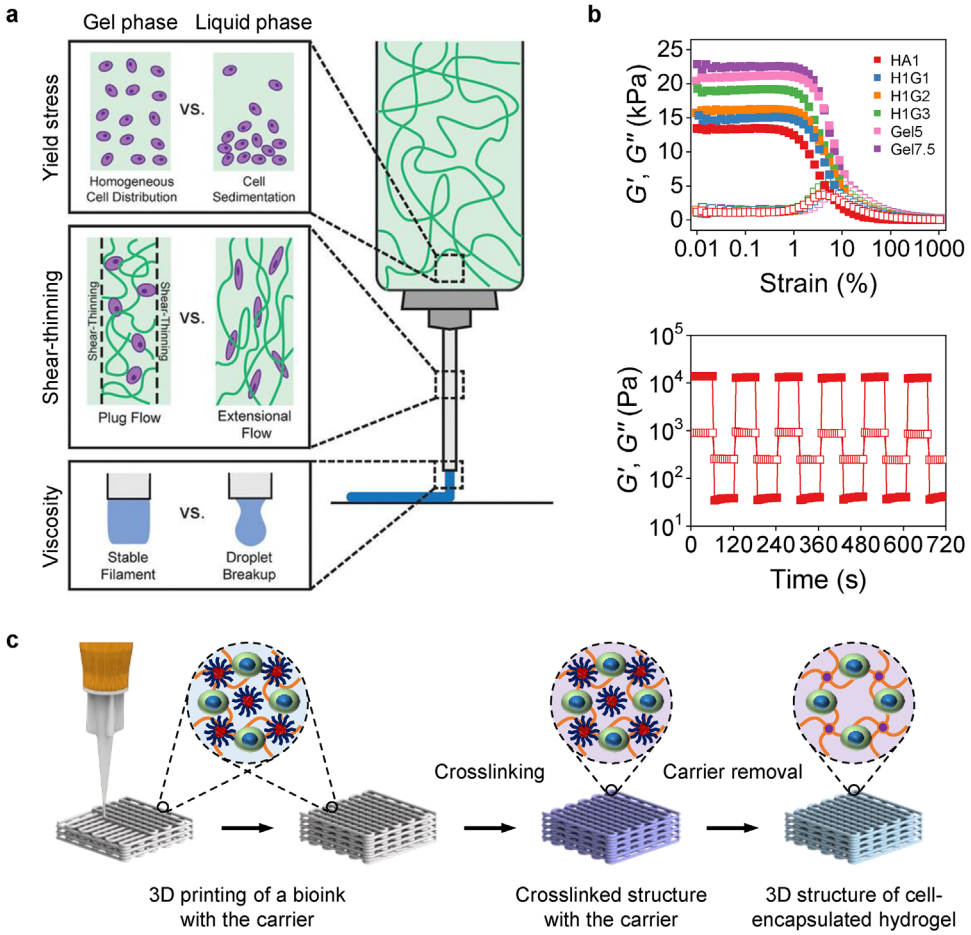

Figure 2. Extrusion-based 3D bioprinting. a) Gel-phase bioinks compared with liquid-phase bioinks. Reproduced with permission.[34] Copyright 2021, Wiley-VCH. b) Shear-thinning (top) and self-healing (bottom) properties of gel-phase bioinks. b, top) G' and G'' of bioinks on oscillatory strain sweeps. HA1: 1 wt% methacrylated hyaluronic acid (HAMA) bioink; H1G1: 1 wt% HAMA and 1 wt% gelatin methacryloyl (GelMA) bioink; H1G2: 1 wt% HAMA and 2 wt% GelMA bioink; H1G3: 1 wt% HAMA and 3 wt% GelMA bioink; Gel5: 5 wt% GelMA bioink; Gel7.5: 7.5 wt% GelMA bioink. b, bottom) Step-strain measurement of a 1 wt% HAMA bioink with oscillatory strain steps between 0.5% and 250%. Solid and open squares represent the shear storage modulus G' and shear loss modulus G'', respectively. c) 3D bioprinting using universal fugitive network bioinks. (b,c) Reproduced with permission.[40] Copyright 2024, American Chemical Society.

properties of the final printed materials.[34] The advantages over other bioprinting modalities include ease of operation and cost-effectiveness.[33] Although the increasing accessibility to affordable extrusion-based bioprinters has driven advancements in this printing method over the past two decades, the limited availability of bioinks remains a critical barrier to progress.[39,40]

Designing bioinks for extrusion-based 3D bioprinting has proven challenging, as they must satisfy several competing requirements.[32–34,39,40] To achieve 3D printability, a bioink must be extrudable, form continuous filaments, and maintain the structural integrity of these filaments after deposition, requiring contradictory characteristics during and after extrusion. To ensure the functionality of printed living constructs, a bioink must protect cells throughout the printing process and provide an environment for cell growth and function within the printed materials. These requirements for 3D printability and cell compatibility oppose each other, introducing the concept of a "biofabrication window" (**Figure 3**).[27,32] For instance, high-viscosity bioinks, which typically have a high polymer content, are preferred for 3D printability. However, such bioinks form dense polymer networks within printed materials, which can limit cell proliferation and functionality. As a result, conventional 3D bioprinting often compromises either 3D printability, including shape fidelity and resolution, or cell compatibility, affecting cell viability and functionality (Figure 3). This tradeoff occurs with both mammalian cells and microbial cells.[20,41] For example, a study on the 3D printing of ELMs composed of *Acetobacter xylinum* (*A. xylinum*) in hyaluronic acid (HA)-based hydrogels showed that increasing the polymer concentration of bioinks improved 3D printability.[41] However, the resulting dense networks of the printed hydrogel matrices reduced the proliferation of *A. xylinum* and its cellulose production due to limited oxygen availability.[41]

A promising strategy to address this challenge for bioink design involves creating gel-phase bioinks with shear-thinning and self-healing properties, which are essential for achieving high-resolution and high-fidelity 3D printing (Figure 2a,b).[34,39,40] The shear-thinning behavior allows bioinks to transition from a

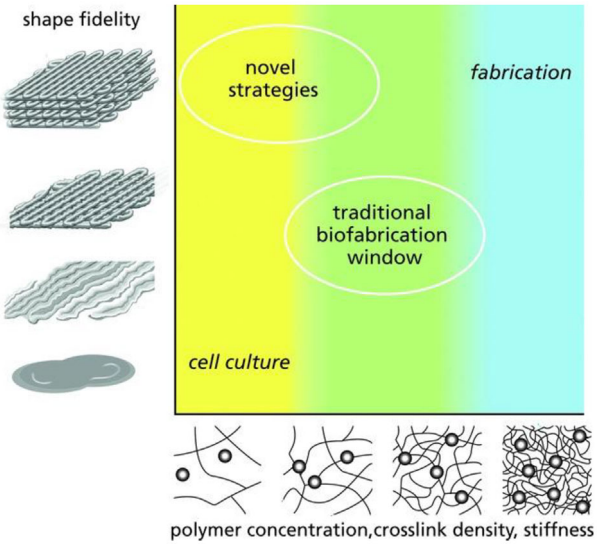

Figure 3. Concept of biofabrication window. Reproduced with permission.[27] Copyright 2013, Wiley-VCH.

solid-like (shear storage modulus $G' >$ shear loss modulus G'') to a liquid-like state ($G' < G''$) under applied stress (e.g., pressure), facilitating bioink extrusion (Figure 2b, top). The self-healing behavior enables the bioinks to recover their solid-like state after shear-thinning-induced extrusion, preventing their spreading upon deposition and thus resulting in high printing fidelity (Figure 2b, bottom). In contrast, liquid-phase bioinks often spread on a substrate upon deposition, impairing printing fidelity and resolution. Additionally, shear-thinning allows for the use of microscale nozzles with low applied stress. This ability is crucial for high-resolution printing and high cell viability and functionality. Printing microscale filaments (e.g., <400 µm) is vital for the viability and functionality of microbial cells due to the limited diffusion of oxygen and nutrients through hydrogel matrices. This is particularly important for printed constructs with high-density aerobic cells. Moreover, lower applied stress for extrusion can enhance the viability of encapsulated cells by reducing the stress exerted on them during bioink extrusion.[33,34,42,43] The plug-like flow driven by shear-thinning can further protect cells, reducing damage during bioink extrusion (Figure 2a).[34,44]

The strategies for designing bioinks with shear-thinning and self-healing behavior include using physical crosslinking, partial pre-crosslinking, and rheology modifiers.[32,34] These approaches have broadened the range of 3D-printable, cell-compatible materials, which are also potentially applicable to the 3D printing of ELMs.[11,41,45–47] For example, gel-phase bioinks with shear-thinning and self-healing behavior have been used for 3D printing ELMs, such as *Pseudomonas putida* (*P. putida*) and *A. xylinum* in HA-based hydrogels,[41] *Escherichia coli* (*E. coli*) and *Saccharomyces cerevisiae* (*S. cerevisiae*) in Pluronic F127 hydrogels,[11,45] and mycelium hydrogels.[47] Although these studies have demonstrated 3D printability, they have not yet incorporated deliberate approaches to customize the physical and biochemical environments within the printed materials for cell functionality and overall ELM performance. Additionally, some studies have demonstrated bioink extrudability without achieving full 3D printability, resulting in low-resolution or non-self-supporting ELM structures, mainly suitable for 2D printing or 3D printing of vertically stacked structures.[20,26,48–52]

These conventional strategies for bioink design, which directly modify the rheological properties of bioink hydrogel precursors, often link these modifications to the physical and biochemical properties of the final printed materials, limiting control over them.[39,40] Moreover, these methods typically require customization for each bioink formulation or only work with specific material systems, hindering the development of bioinks tailored for specific cell types and applications.[39,40]

Generalizable 3D bioprinting strategies are promising for achieving both 3D printability and cell compatibility (Figure 2c). A generalizable approach involves a universal bioink platform, such as complementary network bioinks[39] and universal fugitive network bioinks,[40] applicable to a broad range of hydrogel systems. These bioinks are prepared by loading cells and hydrogel precursors into a 3D-printable fugitive carrier.[39,40] To achieve 3D printability, these approaches rely on the rheological properties of the fugitive carriers, which are removed after printing, rather than those of bioink hydrogel precursors as in conventional bioinks.[39,40] This decoupling of 3D printability of bioinks from the rheological properties of bioink hydrogel precursors expands the applicability of these approaches to a range of hydrogels, including those traditionally considered non-3D-printable and those with low polymer concentrations.[39,40] The decoupling also enables the bioink design for the physical and biochemical properties of the final printed hydrogels—and, therefore, the functionality of the printed living constructs—without compromising 3D printability.[39,40] Because they use a gel-phase carrier with shear-thinning and self-healing properties, these approaches share the advantages of gel-phase bioinks regarding 3D printability and cell viability, as discussed above (Figure 2). Other strategies for achieving both printability and cell compatibility include embedded 3D bioprinting in support baths, which utilizes sacrificial support materials instead of sacrificial printable carriers, as described in Section 2.2.

Previous studies on the 3D bioprinting of ELMs have demonstrated high viability (e.g., >95%)[11,41] and sustained proliferation (e.g., metabolically active for up to 4 months)[46] of microbial cells within printed constructs, including Gram-positive bacteria (e.g., *Bacillus subtilis* (*B. subtilis*)), Gram-negative bacteria (e.g., *P. putida*), and yeast cells.[11,20,41,45,46] These results indicate microbial cell compatibility with commonly used bioink compositions and bioprinting conditions, many of which were initially optimized for mammalian cells. These conditions include printing pressures (below 300 kPa) for bioink extrusion and ultraviolet (UV) light exposure (365 nm for up to several minutes) for crosslinking.[11,20,41,45,46] Furthermore, microbial cells with protective cell walls, such as bacteria and yeast, are more resilient to relatively harsh environments, including shear stress during bioink extrusion and UV irradiation during crosslinking, compared to more susceptible mammalian cells.[11]

2.2. Embedded 3D Bioprinting in Support Baths

Embedded 3D bioprinting in support baths offers an alternative to conventional extrusion-based printing for fabricating 3D

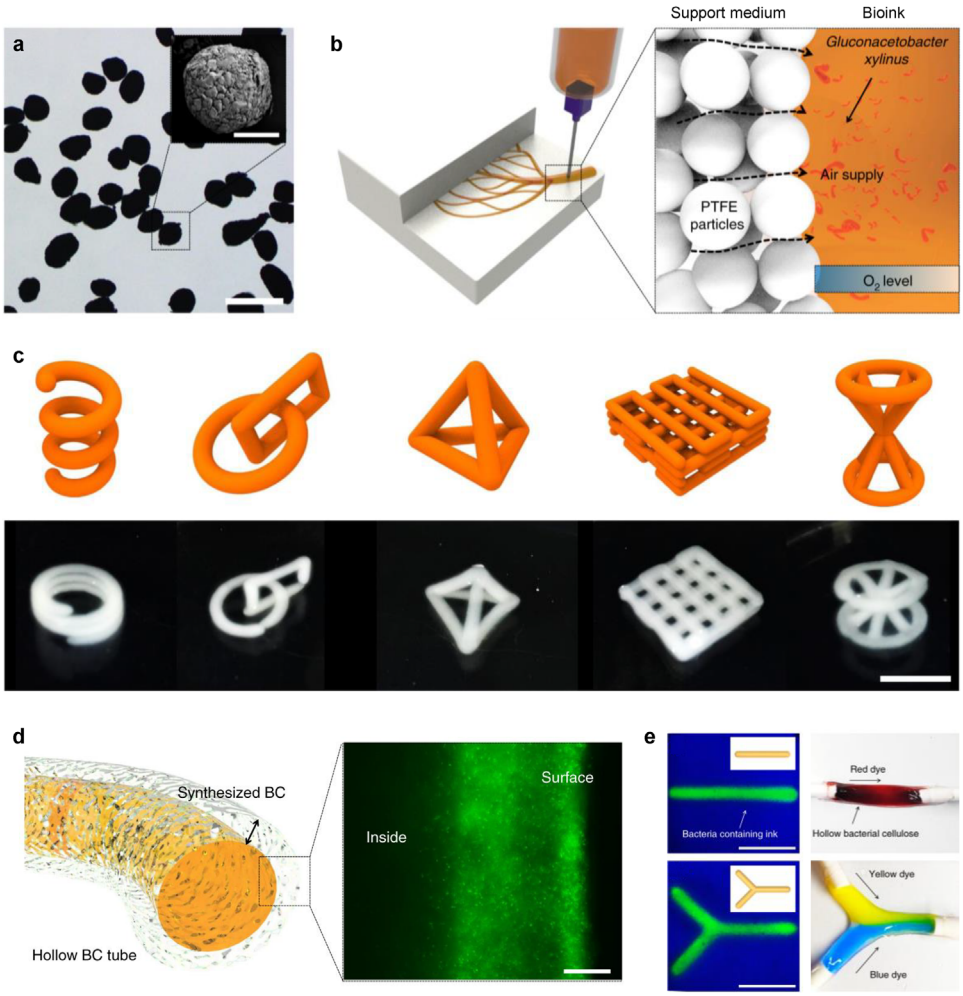

Figure 4. Embedded 3D bioprinting in support baths for the fabrication of BC structures via the in situ biosynthesis of BC by *G. xylinus* within printed filaments. a) Optical microscopy image of polytetrafluoroethylene (PTFE) microparticles used as a support medium with an inset showing an electron microscopy image. Scale bars: 500 µm; 100 µm (inset). b) Schematic of embedded 3D bioprinting using air-permeable microparticle matrices as the support medium. c) 3D models used for printing (top) and 3D-printed structures of cellulose nanofiber (CNF)/BC (bottom). CNF was used as the main component of the matrix in the bioinks. Scale bar: 1 cm. d) Schematic of a hollow BC tube (left) and image of bacteria (green) near the surface of a printed filament after 7 days of incubation (right). Scale bar: 50 µm. e) CNF/BC tubes filled with fluorescent particles (left) and hollow CNF/BC tubes showing the flow of red-colored liquid (right, top) and yellow and blue liquids (right, bottom). Scale bars: 1 cm. Reproduced under terms of the CC-BY license.[53] Copyright 2019, The Authors, published by Springer Nature.

constructs of ELMs (**Figure 4**).[53,54] This approach prints bioinks into a yield-stress medium (support bath) that temporarily supports the printed structures until postprinting crosslinking (Figures 1b and 4a,b).[55–60] The yield-stress behavior allows for the movement of the print nozzle through the medium for bioink extrusion while maintaining the structural integrity of the printed structures. After bioink extrusion, the medium reforms around the printed filaments, supporting their structural integrity during and after printing. The printed structures are then mechanically stabilized within the support bath through crosslinking or reinforcement processes. For ELMs, stabilization can also be achieved through in situ biosynthesis of polymer networks, such as biofilms, by microbial cells.[53,54] Once stabilized, the constructs are extracted from the support bath.

This approach eliminates the need for printed structures to be self-supporting before postprinting crosslinking, reducing the rheological requirements for bioinks. This feature broadens the range of printable materials, including low-viscosity ones that are typically unsuitable for 3D printing. Furthermore, printing in supporting baths allows for the creation of more sophisticated structures with enhanced resolution, as the support medium enables nonplanar layer-by-layer printing and freeform printing, which is challenging for conventional extrusion-based printing in the air (Figure 4c). Additionally, the water-rich, biocompatible environment of the support medium can support cell viability, thereby extending printing time and enabling the fabrication of larger and more complex structures.

Although printing into a support medium reduces the printability requirements for bioinks, the support medium itself must have well-controlled rheological properties for bioink extrusion and deposition, such as yield-stress and self-healing behavior. The medium must also allow for postprinting crosslinking and

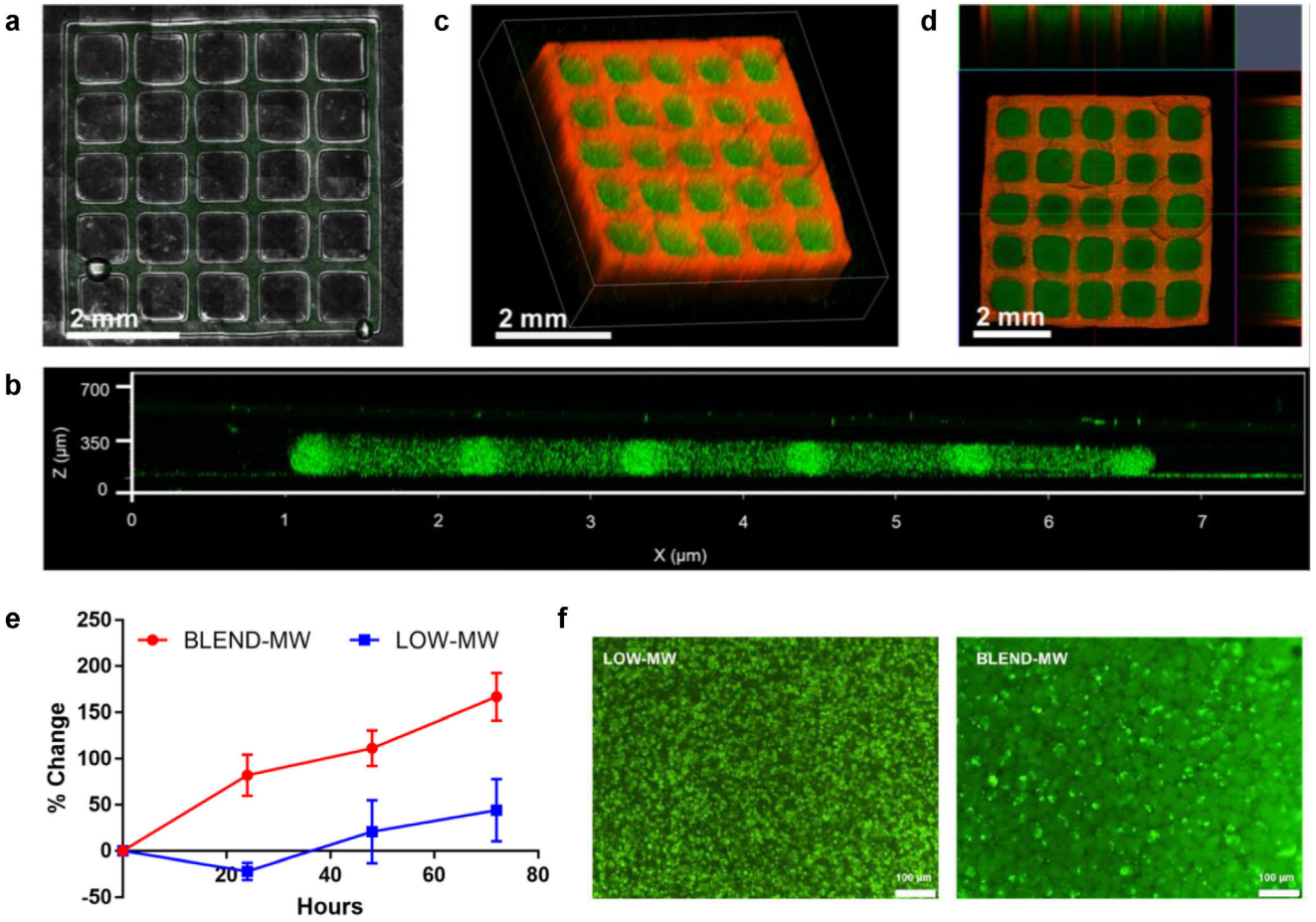

Figure 5. Digital light processing 3D bioprinting of ELMs. a) Top-down view image of a 3D-bioprinted grid structure with *E. coli*. b) Side view confocal z-stack image of the grid structure in (a) with encapsulated *E. coli* expressing green fluorescent protein (GFP). c) Rotated-view confocal z-stack image of a 3D-bioprinted grid structure with two types of *E. coli* expressing either GFP (green) or mCherry (red). d) Top-down view of the grid structure in (c) with side view insets. e) Viable biomass accumulation in ELMs printed using a mixture of low- and high-molecular-weight (MW) PEGDA (BLEND-MW, red) and low-MW PEGDA (LOW-MW, blue) as the hydrogel matrix over time, measured by changes in GFP intensity from *E. coli* expressing GFP. f) Fluorescence images of *E. coli* (green) encapsulated in LOW-MW (left) and BLEDN-MW (right) PEGDA for 72 h. Reproduced under terms of the CC-BY-NC-ND license.[67] Copyright 2021, The Authors, published by American Chemical Society.

the extraction of printed constructs without compromising their structural integrity or damaging cells. In some applications, the medium must be air-permeable to support oxygen-dependent cells, for example, when in situ aerobic biosynthesis is used for postprinting mechanical stabilization within the support bath before extraction (Figure 4b).[53,54] For instance, embedded 3D bioprinting has been used to fabricate bacterial cellulose (BC) structures via the in situ biosynthesis of BC by *Gluconacetobacter xylinus* (*G. xylinus*) within printed materials, using air-permeable microparticle matrices as the support medium (Figure 4).[53,54] In one study, *G. xylinus* produced BC near the surface of printed filaments—at the interface between the filaments and the air-permeable medium—where oxygen levels are high, enabling the fabrication of hollow tubular cellulose structures (Figure 4d,e).[53]

Beyond fabricating 3D constructs, this technique can also be used to create structures with channels by removing the printed filaments but retaining the support medium.[56,57,59,61] This can be achieved by printing a sacrificial ink into a crosslinkable support medium to define channel networks. After printing, the support medium is crosslinked to form a bulk structure, and the sacrificial ink is removed, leaving channels within the structure. Such vascularization strategies are particularly beneficial for large living constructs, where diffusion alone cannot adequately supply oxygen and nutrients to cells throughout the constructs. Although conventional extrusion-based 3D printing can also form channels using sacrificial inks,[62–64] embedded 3D printing in support baths enables the creation of more complex, biomimetic channel networks through omnidirectional printing aided by the support medium.[57,59,61]

2.3. Light-based 3D Bioprinting

Digital light processing (DLP) 3D bioprinting is a promising technique for fabricating complex 3D constructs of ELMs with high throughput and resolution (**Figure 5**). DLP bioprinting uses patterned light (digital light projection) to selectively crosslink light-sensitive liquid bioinks, or bioresins, transforming

them layer by layer into cell-encapsulated 3D structures (Figures 1c and 5).[65–67] DLP enables high-resolution printing down to the micrometer scale, superior to the typical resolution of extrusion-based printing (above 100 μm). This feature allows for the fabrication of intricate architectures that are challenging to achieve with conventional extrusion-based bioprinting.

Unlike extrusion bioprinting, which serially deposits continuous bioink filaments using a print nozzle, DLP prints entire layers simultaneously, rapidly fabricating multiple structures in parallel. This nozzle-free process reduces print time, potentially improving the viability of encapsulated cells during printing. However, DLP requires photocrosslinkable bioinks with rapid crosslinking capabilities and low viscosity (less than 10 Pa•s),[68,69] which limits the range of printable materials and compatible crosslinking mechanisms.

DLP bioprinting has been applied to fabricate 3D constructs of ELMs,[67–69] including engineered *Caulobacter crescentus* (*C. crescentus*) embedded in poly(ethylene glycol diacrylate) (PEGDA),[67] *E. coli* and *S. cerevisiae* in bovine serum albumin (BSA) conjugated with PEGDA,[68] and *S. cerevisiae* in PEGDA (Figure 5).[69] Other light-based bioprinting methods applicable to ELB fabrication include stereolithography,[70,71] two-photon polymerization,[72–74] and laser-assisted bioprinting.[75–79] These methods, such as stereolithography and two-photon polymerization, can achieve even higher resolution than DLP. However, they rely on serial, point-by-point photocrosslinking processes, resulting in slower printing speeds.

2.4. Volumetric 3D Bioprinting

Volumetric additive manufacturing (VAM) is an emerging light-based printing technology that concurrently produces entire 3D objects using optical tomographic projection rather than the layer-by-layer deposition of bioinks (**Figure 6**).[80,81] VAM illuminates a rotating volume of a photosensitive material with a series of 2D light patterns, cumulatively delivering the computed 3D light dose required to form the target geometry (Figures 1d and 6).[80,81] This layerless approach offers several advantages over traditional layer-based 3D printing methods. These advantages include rapid and scalable printing (e.g., 30 to 120 s for centimeter-scale objects), printing 3D structures around preexisting objects, printing hollow or overhanging features without support structures, and smooth surface finishes.[80,81] However, because the volume of bioink must exceed that of the final printed construct, VAM requires a large volume of bioink. This limitation restricts its application with high-cost materials or the fabrication of large constructs, which are constrained by the size of the bioink container.

Building on VAM, volumetric bioprinting (VBP) has been developed to create hydrogel-based constructs containing cells and organoids (Figure 6).[82–87] Furthermore, because VBP uses a bioink bath, it can be seamlessly integrated with embedded 3D bioprinting in support baths, enabling the fabrication of multimaterial constructs (Figure 6).[86,87] This integration allows the encapsulation of 3D structures printed by extrusion bioprinting within a VBP-formed 3D object. VBP offers the potential to rapidly produce geometrically complex, large-scale ELM constructs, complementing other 3D bioprinting methods.

Chemicals and materials: anhydrotetracycline (aTc), bisacrylamide (BIS), bisphenol A (BPA), cellulose nanocrystal (CNC), fumed silica (FS), glycidyl methacrylate hyaluronic acid (GMHA), isopropyl β-D-1-thiogalactopyranoside (IPTG), κ-carrageenan (κ-CA), MHET (mono(2-hydroxyethyl) terephthalic acid), *N*-acyl homoserine lactone (AHL), Pluronic F127-diacrylate (F127-DA), Pluronic F127-dimethacrylate (F127-DMA), rhamnose (Rham).

3. Current Challenges and Potential Opportunities

3.1. Understanding the Interactions between Living and Nonliving Components of ELMs for Bioink Design

Advancing 3D printing of functional ELMs requires cohesive integration of their living (microbial cells) and nonliving (hydrogel matrices) components. This integration demands two critical efforts: (1) understanding the interactions between microbial cells and hydrogel matrices and (2) designing bioinks based on this knowledge to ensure both the 3D printability of bioinks and the functionality of printed ELM constructs.

Understanding how hydrogel matrices influence microbial behavior is crucial for achieving the desired functionality of ELMs. The physical, structural, and biochemical properties of hydrogel matrices affect not only the viability and proliferation of microbial cells but also their behavior, including motility, morphology, organization, signaling, metabolism, and responsiveness.[4,5,20,53,88–91] For example, the densities of polymer networks and crosslinks regulate the diffusion of nutrients and oxygen through hydrogel matrices, controlling microbial growth and metabolism .[41,69] In one study, as the density of hydrogel matrices increased, ELMs composed of *A. xylinum* encapsulated in hyaluronic acid-based hydrogels showed decreased proliferation, cellulose production, and growth depth due to limited oxygen availability.[41] Similarly, another study using betaxanthin-producing *S. cerevisiae* encapsulated in PEGDA hydrogels reported that increasing the PEGDA concentration reduced the number and density of colonies, thereby decreasing the production of betaxanthins.[69] Increasing the concentration of cellulose nanofiber, the primary matrix component, in bioinks also reduced the bacterial cellulose production of *G. xylinus*.[53] Moreover, *E. coli* cells encapsulated in a mixture of low- and high-MW PEGDA formed larger, overlapping colonies and exhibited higher proliferation, whereas those in low-MW PEGDA formed smaller, discrete colonies (Figure 5e,f).[67]

More importantly, the material properties of hydrogel matrices can influence the gene expression profiles, metabolic pathways, adaptive activities, and intercellular interactions of microbial cells—factors that remain largely unexplored.[5,92–94] Understanding the interplay between encapsulated cells and their local environments could make the nonliving component of ELMs (hydrogel matrices) an effective tool for controlling the behavior of their living component (microbial cells) and, consequently, the overall functionality of these materials.

Building on this understanding, the next step is to design bioinks capable of creating physical and biochemical environments tailored to specific cell types and their functionality within

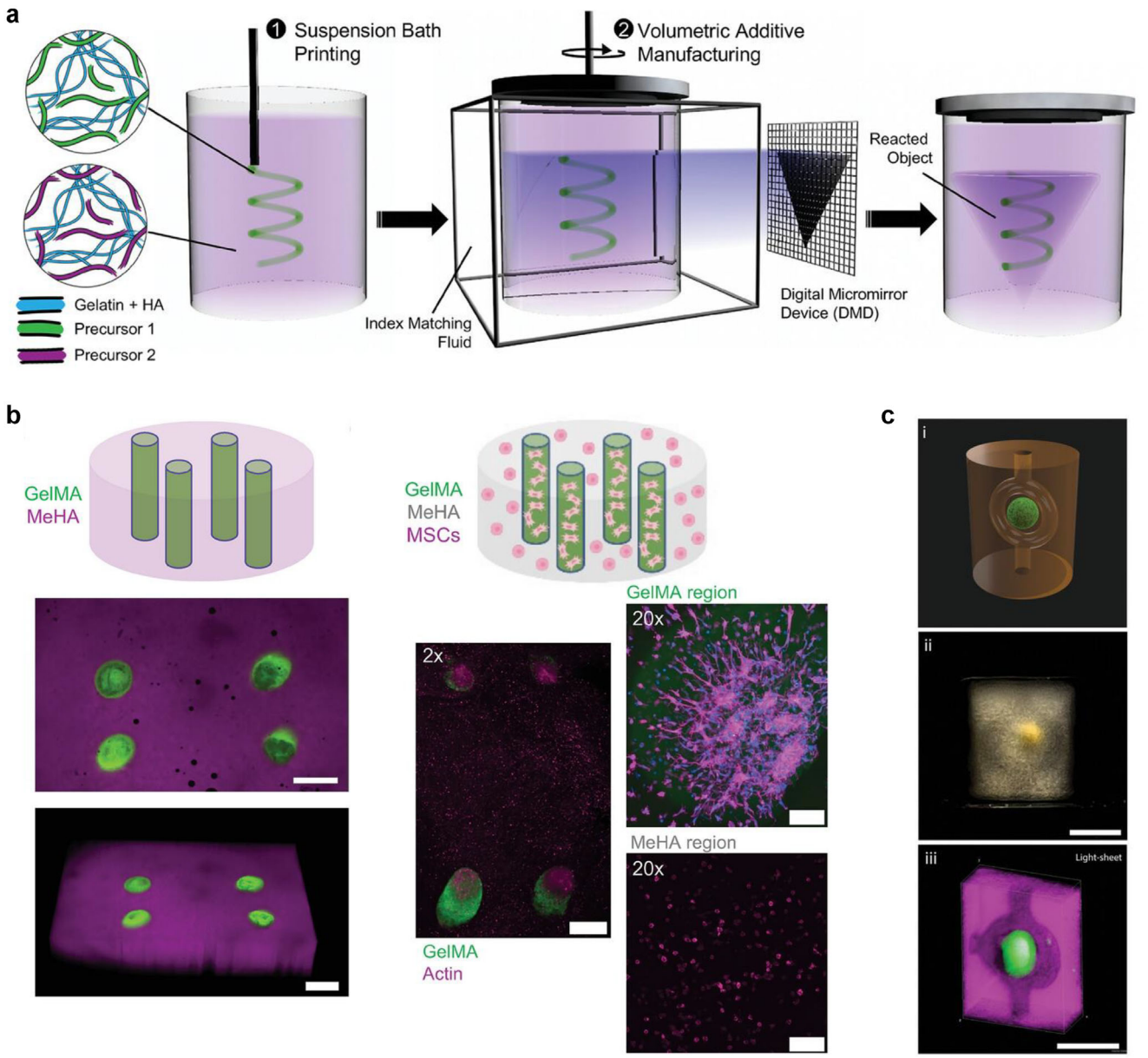

Figure 6. Volumetric 3D bioprinting. a) Sequential suspension bath printing (embedded printing in support baths) and volumetric printing. b) Schematics (top) and images (bottom) of multimaterial constructs printed via sequential embedded and volumetric printing: acellular construct (left) and cellular construct (right) containing methacrylated hyaluronic acid (MeHA, purple) and gelatin methacryloyl (GelMA, green) regions. Mesenchymal stromal cells (MSCs) are encapsulated in the construct (right). Scale bars: 1 mm (left); 2x: 1 mm, 20x: 150 µm (right). (a,b) Reproduced with permission.[87] Copyright 2024, Wiley-VCH. c) 3D construct fabricated by sequential embedded and volumetric printing: (i) 3D model, (ii) stereomicrograph image, and (iii) light-sheet scan reconstruction. Scale bars: 4 mm (ii); 6 mm (iii). Reproduced under terms of the CC-BY license.[86] Copyright 2023, The Authors, published by Wiley-VCH.

printed ELMs. As discussed earlier, developing such bioinks for extrusion-based bioprinting is challenging due to conflicting requirements for 3D printability and cell compatibility. A promising strategy is generalizable 3D bioprinting using a universal bioink platform (Figure 2c).[39,40] This approach decouples the printability of bioinks from the rheological properties of bioink hydrogel precursors, allowing independent control over their compositions and, thus, the physical and biochemical properties of the final printed matrices. Its generalizable printability can also facilitate high-throughput screening of bioinks (hydrogel base materials) with varying chemical compositions, polymer network densities, and crosslinking structures, enabling the design of bioinks customized for specific functional needs within printed ELMs.

Furthermore, the integration of machine learning[95–98] and high-throughput experimentation[99–101] has the potential to shift the paradigm in bioink design. This data-driven approach can significantly enhance the prediction of

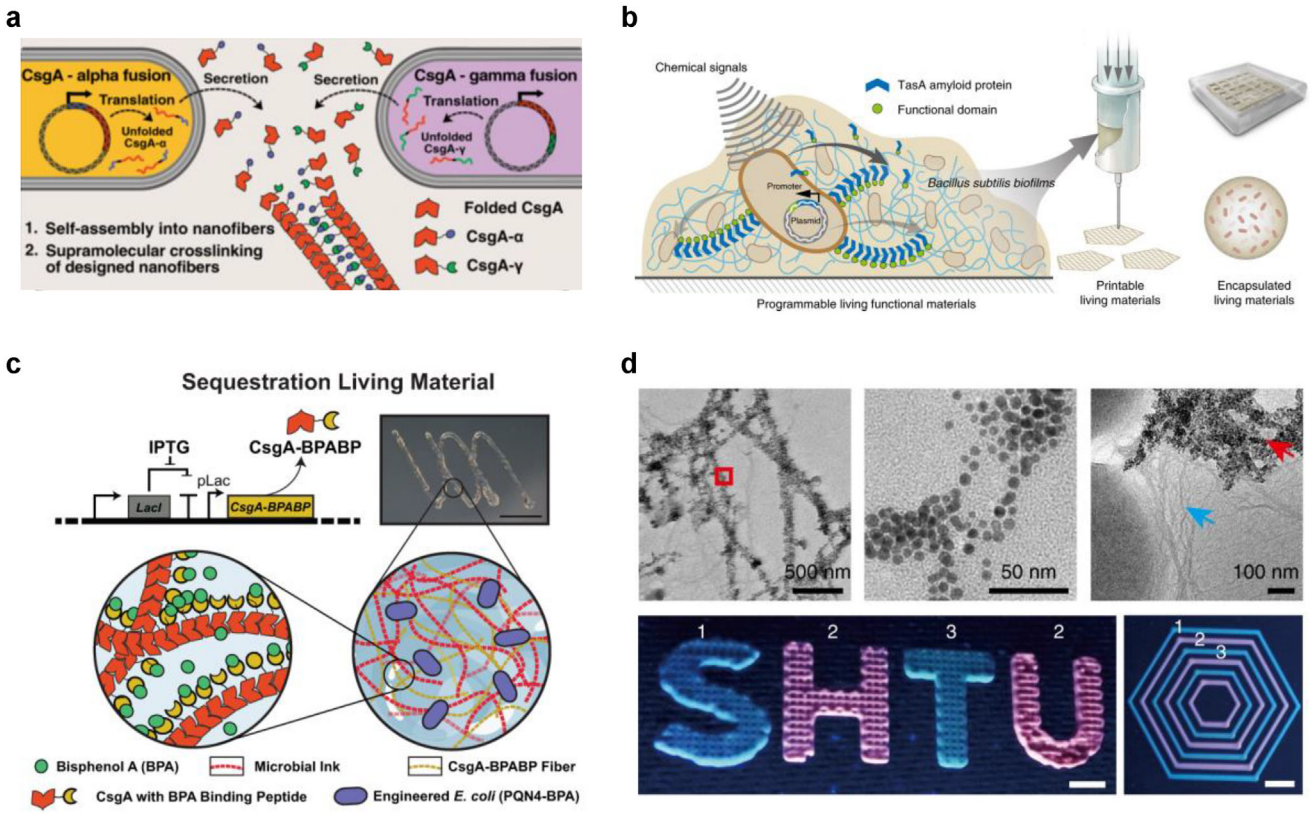

Figure 7. Synthetic biology for 3D bioprinting of engineered living constructs. a,b) Synthetic biology for bioink design and production. Examples include microbial biofilm-based inks produced using (a) CsgA fusion proteins secreted by genetically engineered *E. coli* and (b) TasA amyloid fusion proteins secreted by genetically engineered *B. Subtilis*. c,d) Synthetic biology for bio-augmented 3D bioprinting. (c) Genetic design of *E. coli* (PQN4-BPA) engineered to produce CsgA nanofibers with BPA-binding peptides (CsgA-BPABP) (top left), an image of a printed living material (top right), and a microbial bioink containing CsgA-BPABP biofilm to print a living material for sequestering BPA (bottom). Scale bar: 5 mm. (d) Transmission electron microscopy (TEM) images of TasA nanofibers conjugated with gold nanoparticles (top) and digital photographs of printed *B. Subtilis* biofilms with three types of immobilized quantum dots (QDs) under UV light: (1) blue QDs, (2) green QDs, and (3) red QDs (bottom). Scale bars: 5 mm (bottom). (a,c) Reproduced under terms of the CC-BY license.[51] Copyright 2021, The Authors, published by Springer Nature. (b,d) Reproduced with permission.[49] Copyright 2018, The Authors, under exclusive license to Springer Nature America, Inc., published by Springer Nature.

interactions between microbial cells and hydrogel matrices and facilitate the design of bioinks tailored to specific cell types, their functions, and the target properties and applications of ELMs. However, the small size of available datasets remains a key obstacle. To accelerate progress, future efforts must focus on establishing standardized experimental and data collection protocols, advancing high-throughput methodologies, and generating high-quality, standardized datasets.

3.2. Synthetic Biology for 3D Bioprinting of Engineered Living Constructs

3.2.1. Synthetic Biology for Bioink Design and Production

Beyond enabling the programmable functionalities of ELMs, synthetic biology offers transformative potential in bioink design (**Figure 7**). By harnessing the ability of microbial cells to produce extracellular polymeric substances for biofilm formation,[93,94,102] novel bioink base materials for hydrogel matrices can be developed. These bioinks are particularly advantageous as they provide a native extracellular matrix (ECM)-like environment for microbial cells within printed materials.

The examples include extrudable microbial inks prepared entirely from biofilms produced by genetically engineered *E. coli* (Figure 7a).[51] This was achieved using two types of *E. coli* cells engineered to secrete CsgA fusion proteins with the alpha-chain ("knob") and gamma-chain ("hole") domains of fibrin.[25,51,102,103] In co-culture, the secreted CsgA-α and CsgA-β proteins self-assembled into curli nanofibers (CsgA-$\alpha\beta$), crosslinked through noncovalent interactions between the knob and hole domains. These nanofibers formed shear-thinning hydrogels suitable for extrusion. Compared with hydrogels formed with either CsgA-α or CsgA-β alone, the CsgA-$\alpha\beta$ hydrogels exhibited improved mechanical properties and printability. Microbial bioinks incorporating genetically engineered microbial cells within these hydrogels were subsequently used to print functional living constructs capable of releasing an anticancer drug (azurin), sequestering a toxic chemical (BPA), and regulating cell growth within the structures. Another study utilized the TasA amyloid machinery of *B. subtilis* to develop biofilm-based bioinks (Figure 7b).[49]

In this case, *B. subtilis* was engineered to express TasA amyloid fusion proteins with diverse functional domains. The secreted proteins self-assemble into fibrous networks integrated with microbial cells, forming biofilms with shear-thinning behavior. Genetic engineering of TasA fusion proteins also enabled tuning the viscoelastic properties of the biofilms, enhancing their printability.

Although further advancements are needed to improve the 3D printability of these microbial bioinks, these approaches hold significant potential for bioink development. Unlike traditional bioinks based on synthetic or nonmicrobial natural polymers, biofilm-based bioinks can create ELMs with microbial cells embedded in native ECM-like matrices, potentially enhancing cell growth and functionality. Moreover, this design approach could enable bioinks with tunable material properties and functions through genetic engineering, support on-demand bioink production in resource-limited environments, and promote sustainable additive manufacturing.[49,51]

3.2.2. Synthetic Biology for Bio-Augmented 3D Bioprinting

In addition to the design and preparation of microbial bioinks, the ability of engineered microbial cells to produce materials introduces novel manufacturing capabilities for 3D bioprinting. Genetically engineered microbial cells encapsulated in bioinks can form secondary polymer networks of extracellular polymeric substances within 3D-printed ELMs, augmenting their material properties. This in-situ production can enhance the mechanical properties of 3D-printed ELMs, enable stimuli-responsive control of their physical characteristics, and introduce advanced functionalities, such as self-healing. Furthermore, pre- or postprinting production of fusion proteins (e.g., CsgA and TasA) with functional peptide domains can impart nonbiological functionalities to 3D-printed ELMs (Figure 7c,d).[25,49,51,102,103] For example, these proteins can interface with inorganic nanomaterials, such as gold nanoparticles and quantum dots, to provide additional capabilities, such as electrical conductivity and environmentally responsive electrical switching (Figure 7d).[49,102]

Beyond biofilm engineering, other chemical substances produced by microbial cells can incorporate new properties and functions into ELMs. For instance, L-DOPA produced by engineered *E. coli* within 3D-printed ELMs increased their mechanical stiffness, while betaxanthins secreted by *S. cerevisiae* enhanced resistance to enzymatic degradation.[68] These examples of postprinting bio-augmentation illustrate the potential of synthetic biology to expand the functional versatility of 3D-printed ELMs.

3.3. Postprinting Growth of 3D-Printed Living Constructs as a Fabrication Process

Incorporating microbial growth into 3D bioprinting enables postprinting manufacturing processes that leverage the "livingness" of encapsulated microbial cells (**Figure 8**). Unlike traditional 3D printing, which produces static structures, these processes allow printed constructs to evolve or grow over time, modifying their properties and morphology in response to environmental conditions.

A notable example is the 3D printing of fungal mycelium hydrogels that support postprinting mycelial growth (Figure 8a).[47] After printing, the mycelium grows, colonizing the printed construct, filling gaps, and reinforcing its structure (Figure 8b,c). This growth process dynamically adapts to environmental factors such as nutrient availability. In nutrient-rich environments, the mycelium shows a slow, highly branched growth pattern (phalanx strategy), while in nutrient-poor environments, it shifts to an exploration growth pattern, extending its networks to seek resources (guerrilla strategy). Beyond geometrical modification and mechanical reinforcement, postprinting growth introduces self-healing capabilities, as the mycelium can grow across cracks or damaged areas in printed constructs, restoring mechanical integrity without external intervention (Figure 8d).

Incorporating microbial growth as a manufacturing process could introduce a new paradigm in 3D bioprinting by enabling the fabrication of evolutionary living constructs. These constructs can grow and adapt to their environments, offering autonomous features such as mechanical reinforcement, environmental responsiveness, and self-healing.

3.4. Integration of Shape-Morphing Materials with 3D Bioprinting of ELMs

Integrating shape-morphing materials with 3D bioprinting can create living constructs with adaptive and dynamic morphologies. This approach, known as 4D printing, involves printing 2D or 3D structures that transform into programmed 3D shapes over time (**Figure 9**). Initially introduced with a focus on building design and construction,[104] this concept has been adapted for 2D and 3D printing of stimuli-responsive hydrogels, facilitating the fabrication of bioinspired 3D structures.[105–109]

A pioneering study in biomimetic 4D printing used extrusion-based 3D printing to fabricate bilayer hydrogel structures with localized anisotropic swelling (Figure 9a,b).[105] The anisotropic swelling and stiffness were achieved by aligning cellulose fibers in the inks along the printing direction (Figure 9a, left). In a bilayer structure, differential swelling between the top and bottom layers, controlled through 3D printing, enabled independent manipulation of the Gaussian and mean curvatures, transforming the structure into a target 3D shape upon swelling in water (Figure 9a, right). This study demonstrated the potential of 4D printing to create biomimetic structures with intricate morphologies, such as plant-inspired 3D constructs (Figure 9b).[105] Another example using extrusion-based 3D printing leveraged anisotropic hydrogel elements—analogous to biological linear contractile elements—as building blocks to fabricate 3D constructs with programmed morphology and motion.[106] The metric incompatibility of an orthogonally growing bilayer structure composed of anisotropic hydrogel elements induced a saddle-like shape. This shape transformation was further harnessed to generate diverse bioinspired morphologies and motions, including bending, coiling, and twisting, mimicking those observed in biological organisms.

Inspired by biological morphogenesis, another approach for 4D printing has encoded thin hydrogel sheets (2D hydrogels) with spatially controlled in-plane growth (expansion or

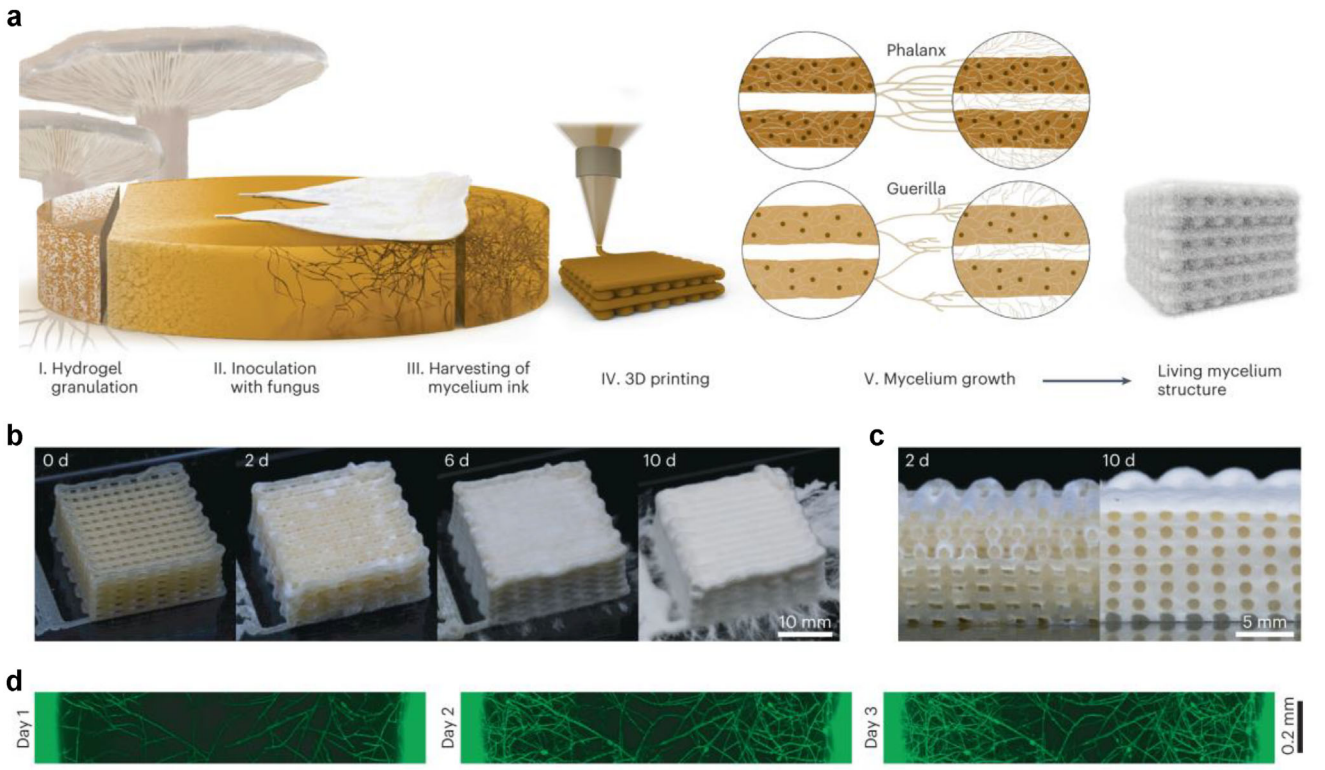

Figure 8. Postprinting growth of 3D-printed living constructs. a) 3D printing of living mycelium structures that support postprinting mycelial growth through the phalanx or guerrilla strategy, depending on nutrient availability. b) Growth of 3D-printed mycelium structures over growth days. c) Cross section of the printed structure after two and ten-day incubation. d) Livingness and self-generation of mycelium structures: microscopy images of mycelia (green) growing between two printed filaments over growth days. Reproduced with permission.[47] Copyright 2022, The Authors, under exclusive license to Springer Nature Limited, published by Springer Nature.

contraction) through photopatterning (Figure 9c).[107–109] The internal stresses generated by differential growth drive the transformation of encoded 2D hydrogels into programmed 3D shapes with defined Gaussian curvatures via out-of-plane deformation.[107–109] This approach has enabled the fabrication of hydrogel structures with complex, doubly curved morphologies observed in living organisms, which are challenging to achieve using conventional methods (Figure 9c). The approaches mentioned above could be extended to the 4D printing of ELMs by utilizing stimuli-responsive hydrogel matrices as active shape-morphing components.

In addition to hydrogel matrices, microbial cells within ELMs can function as active components for shape transformation in 4D printing (**Figure 10**). For instance, the proliferation of *S. cerevisiae* or *S. boulardii* within ELMs induced volume changes, enabling shape morphing.[52,110] Spatial regulation of cell proliferation via photopatterning with UV light (Figure 4a,b) or extrusion-based printing (Figure 4c,d) led to differential volume changes, resulting in controlled 2D-to-3D shape transformations. Genetic engineering of these yeast cells also enabled volume changes in response to specific amino acids, nucleotides, or blue light, supporting spatiotemporally controlled molecule- and light-responsive shape transformations.[52,110] These yeast cells proliferated and functioned for up to 120 h in a medium containing yeast extract, peptone, and D-glucose (YPD) at 30 °C.[52,110] Integrating genetically engineered microbial cells as active components allows shape-morphing constructs to exhibit highly specific and sensitive responses to diverse physical and biochemical stimuli—capabilities that are difficult to achieve with synthetic stimuli-responsive materials.[111] Likewise, mammalian cells have been utilized as active components in shape-morphing constructs, such as soft robots, by harnessing their contractile forces to generate movement and shape change.[112–116]

The 4D printing of ELMs can utilize microbial cells or hydrogel matrices as active components for shape transformation, introducing bioinspired morphologies and shape-morphing capabilities into ELMs. These developments could expand the applications of ELMs to dynamic, responsive engineering systems, including specific-molecule-responsive drug delivery systems and soft biohybrid actuators and robots.[52,110,111]

4. Outlook

The integration of ELMs with 3D bioprinting can transform these materials into living constructs with customizable geometries and programmable functionalities while introducing new manufacturing capabilities for 3D bioprinting. Research at the interface of these two emerging technologies can synergize the biological programmability of ELMs with the geometry-driven functionality of 3D-printed constructs, significantly expanding their technological applications. This convergence can also enable a new paradigm of "living" additive manufacturing that leverages

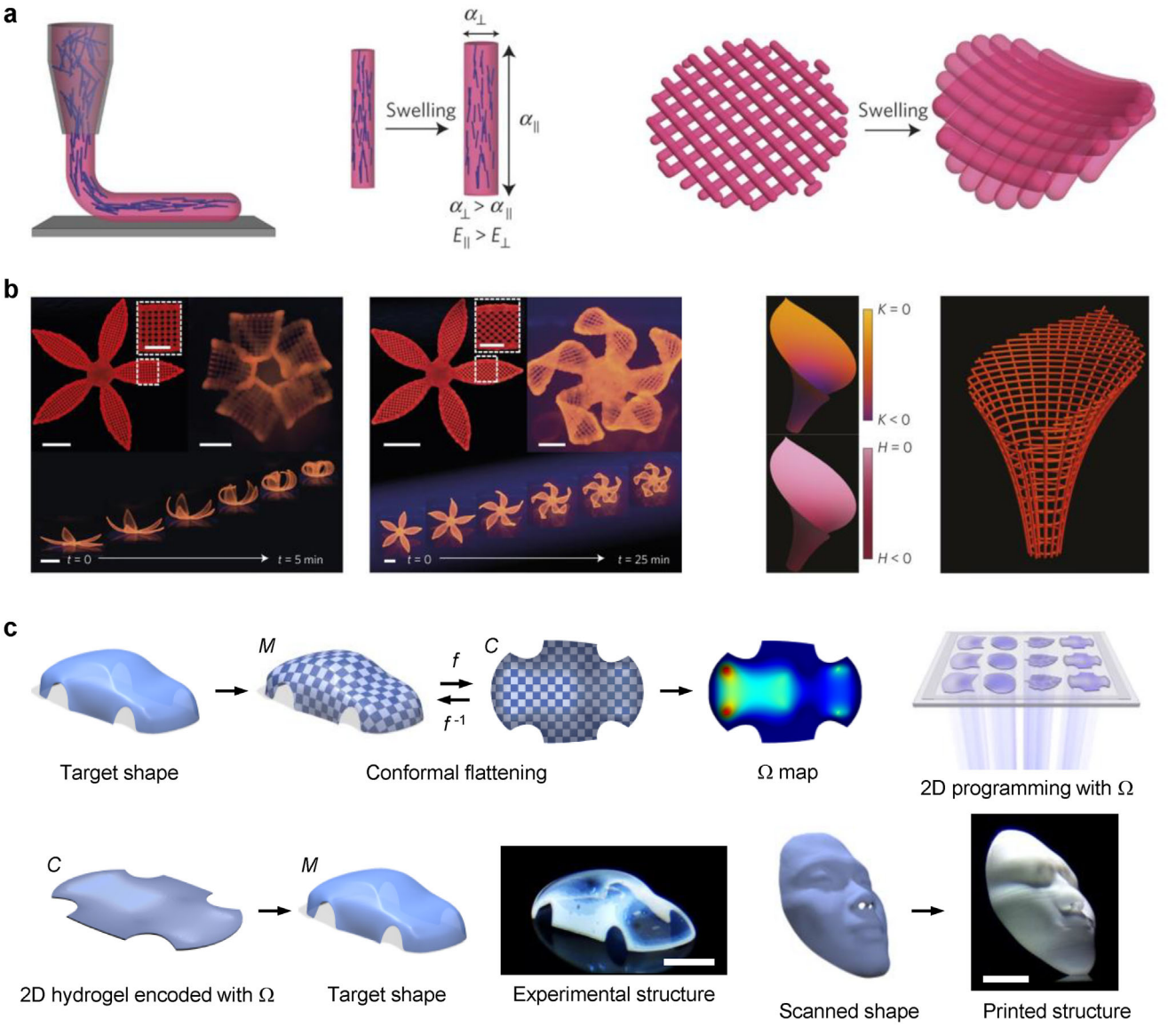

Figure 9. 4D printing. a) Schematic of extrusion-based biomimetic 4D printing. The shear-induced alignment of cellulose fibers leads to anisotropic stiffness E and swelling strain α (left). Differential swelling in bilayer structures enables independent control of the Gaussian K and mean H curvatures, transforming these structures into programmed 3D morphologies (right). b) Complex flower morphologies generated by biomimetic 4D printing in (a). Scale bars: 5 mm, 2.5 mm (inset). (a,b) Reproduced with permission.[105] Copyright 2016, Springer Nature. c) Digital light 4D printing: 2D material programming for 3D shaping. This approach translates a 3D target shape M into 2D growth Ω via conformal mapping f of M to the plane C (f: $M \rightarrow C$) (top, left) and encodes 2D hydrogels with Ω using digital light projection grayscale lithography (top, right). The 2D hydrogels encoded with Ω transform into programmed 3D shapes (bottom). Scale bars: 4 mm (left), 5 mm (right). Reproduced under terms of the CC-BY license.[109] Copyright 2021, The Authors, published by Springer Nature.

the "livingness" of microorganisms as an active element in the manufacturing process. Such an approach can create 3D living constructs capable of growing or evolving in response to external environments, akin to biological organisms.

Emerging studies on the 3D bioprinting of ELMs have demonstrated enhanced functionality for potential biomedical,[26,41,53] environmental,[20,41,67] and industrial biomanufacturing[46] applications. In biomedicine, customizable 3D-printed ELMs enable the creation of personalized constructs, such as artificial blood vessels, tissue scaffolds, and wound-shaped, antibiotic-producing patches.[26,41,53] For environmental applications, printed grid geometries of ELMs improve bioremediation efficiency, such as phenol degradation, metal sequestration, and pollutant decontamination, by increasing the surface area-to-volume ratio and enhancing mass transport, outperforming bulk ELMs.[20,41,67] In industrial biomanufacturing, 3D-printed lattice structures of ethanol-producing yeast ELMs, featuring microscale filaments and channels, significantly improve mass-transfer efficiency, including nutrient supply and waste removal, and increase the surface area at the ELM–medium interface, both of which are

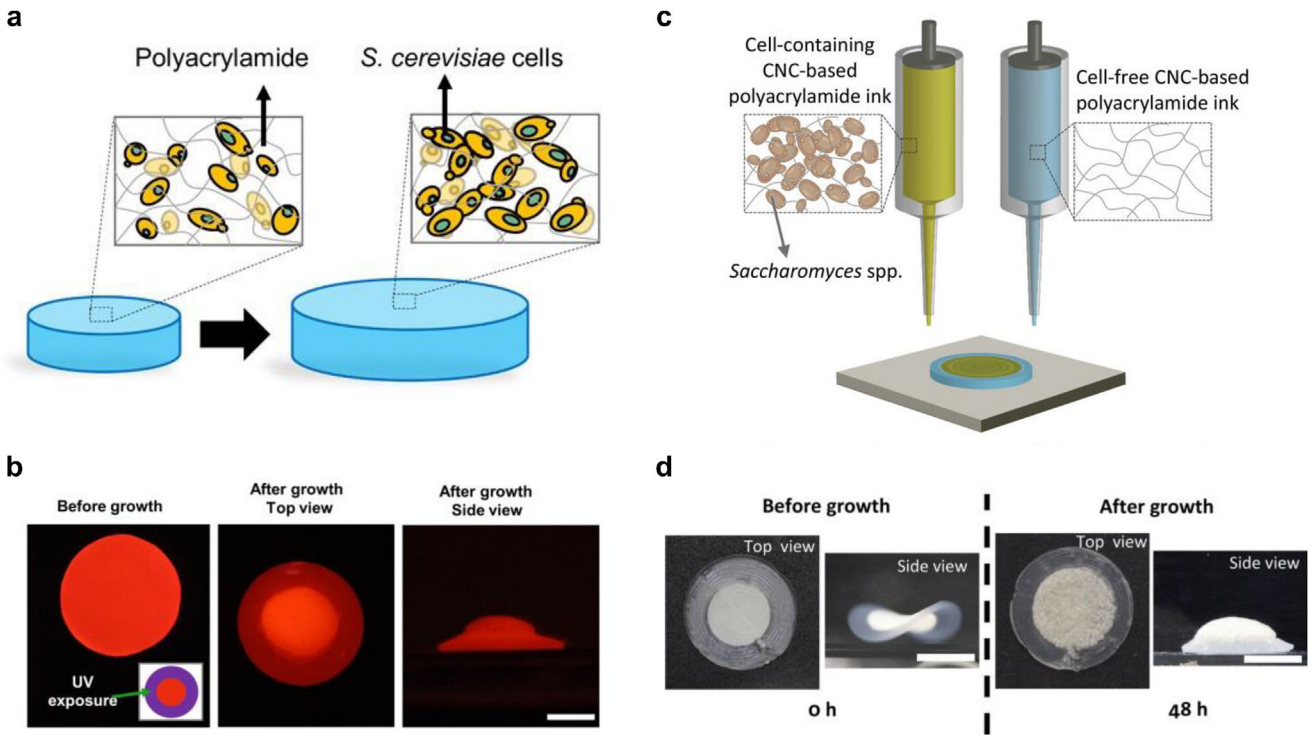

Figure 10. Integration of shape-morphing materials with 3D bioprinting of ELMs: 4D printing using microbial cells within ELMs as active components driving shape transformation. a) Volume expansion of an ELM induced by the proliferation of *S. cerevisiae*. b) Shape morphing of a flat ELM into a hat-like structure, driven by spatially controlled cell proliferation. The spatial control of cell proliferation was achieved using patterned UV light irradiation, which selectively kills cells. Scale bar: 5 mm. (a, b) Reproduced under terms of the CC-BY license.[110] Copyright 2020, The Authors, published by The American Association for the Advancement of Science. c) Printing of a multimaterial shape-morphing ELM. d) Shape morphing of an ELM composed of a cell-containing inner area and a cell-free outer area. The ELM transforms into a hat-like structure driven by cell growth within the inner area. Scale bars: 10 mm. Reproduced with permission.[52] Copyright 2021, Wiley-VCH.

critical for high-cell-density ELMs.[46] These geometries result in a several-fold increase in ethanol production compared to solid constructs.[46] Moreover, multimaterial bioprinting enables the fabrication of multifunctional ELMs with advanced capabilities, such as logic gate-based computation and spatiotemporal responses to multiple molecular signals.[11]

As the unique features of ELMs primarily rely on viable cells, addressing two critical challenges is essential for real-world applications: maintaining cell viability within 3D-printed ELMs and ensuring their safety during and after use. Overcoming these challenges will require convergent approaches that integrate the living and nonliving components of ELMs, building on recent advances in synthetic biology, materials science, and 3D bioprinting. Cell viability can be improved by engineering robust microbial strains through synthetic biology. In addition, designing matrices or bioinks tailored to specific cell types and applications can protect cells in target environments while supporting their growth and functionality. These efforts can be further facilitated by leveraging extensive research in 3D bioprinting with mammalian cells, tissue engineering, and polymeric materials over the last decades. Biosafety can be addressed through robust containment strategies that combine biochemical and physical measures. Biocontainment strategies, such as the use of genetically engineered kill switches, can prevent the unintended propagation of genetically engineered cells in the environment.[117–119] Physical containment, achieved by encapsulating microbial cells within ELM matrices, can provide additional safeguards against microbial escape.[35–38] This strategy can be further enhanced by integrating recent advancements in the bioink design for mammalian cells and hydrogel matrices into the 3D bioprinting of ELMs.

Early developments have demonstrated the effectiveness of these strategies, primarily within the distinct domains of synthetic biology, materials science, and 3D bioprinting. Moving forward, interdisciplinary collaboration among synthetic biologists, materials scientists, and additive manufacturing researchers will be crucial to overcoming cell viability and biosafety challenges and unlocking the full potential of 3D bioprinting of ELMs for practical applications.[120]

Moreover, several broader challenges must be addressed to enable the successful commercialization of ELM technologies. First, the biocontainment of genetically modified organisms (GMOs) or engineered microbiota must be ensured to prevent any unintended environmental or health impacts from their release. Second, live cells must maintain their viability and functionality throughout material processing and at the application site. Third, while proof-of-concept demonstrations have been achieved at the laboratory scale, the scalable production of ELMs for commercial deployment remains unrealized, requiring consideration of both economic and environmental factors.

Finally, as the adoption of ELMs continues to grow, establishing comprehensive regulatory frameworks will be critical to managing their technological, social, ethical, and environmental impacts. These frameworks will foster the responsible innovation of ELMs and ensure their secure and sustainable application. Given the involvement of live cells in ELMs, often genetically engineered, governments are likely to apply regulations similar to those for GMOs, although commercialization of ELMs is still in its early stages. Because the release of GMOs into the environment is a major concern, robust biocontainment strategies must be integrated into ELM development. In addition, the stability of engineered cells and their functions within materials must be maintained in a reproducible and economically viable manner to successfully translate this nascent technology into the market.

Acknowledgements

The authors acknowledge support from the National Science Foundation (OISE-2435184, T.S.M. and DMR-1848511 and DMR-2425164, K.Y.).

Conflict of Interest

The authors declare no conflict of interest.

Keywords

3D bioprinting, 4D printing, engineered living materials, synthetic biology

Received: January 10, 2025
Revised: March 27, 2025
Published online:

[1] P. Q. Nguyen, N.-M. D. Courchesne, A. Duraj-Thatte, P. Praveschotinunt, N. S. Joshi, *Adv. Mater.* **2018**, *30*, 1704847.
[2] C. Gilbert, T. Ellis, *ACS Synth. Biol* **2019**, *8*, 1.
[3] T.-C. Tang, B. An, Y. Huang, S. Vasikaran, Y. Wang, X. Jiang, T. K. Lu, C. Zhong, *Nat. Rev. Mater.* **2021**, *6*, 332.
[4] A. Rodrigo-Navarro, S. Sankaran, M. J. Dalby, A. del Campo, M. Salmeron-Sanchez, *Nat. Rev. Mater.* **2021**, *6*, 1175.
[5] X. Liu, M. E. Inda, Y. Lai, T. K. Lu, X. Zhao, *Adv. Mater.* **2022**, *34*, 2201326.
[6] A. P. Liu, E. A. Appel, P. D. Ashby, B. M. Baker, E. Franco, L. Gu, K. Haynes, N. S. Joshi, A. M. Kloxin, P. H. J. Kouwer, J. Mittal, L. Morsut, V. Noireaux, S. Parekh, R. Schulman, S. K. Y. Tang, M. T. Valentine, S. L. Vega, W. Weber, N. Stephanopoulos, O. Chaudhuri, *Nat. Mater.* **2022**, *21*, 390.
[7] D. E. Cameron, C. J. Bashor, J. J. Collins, *Nat. Rev. Microbiol.* **2014**, *12*, 381.
[8] F. Sedlmayer, D. Aubel, M. Fussenegger, *Nat. Biomed. Eng.* **2018**, *2*, 399.
[9] S. M. Brooks, H. S. Alper, *Nat. Commun.* **2021**, *12*, 1390.
[10] C. Xi, J. Diao, T. S. Moon, *Cell Systems* **2023**, *14*, 1024.
[11] X. Liu, H. Yuk, S. Lin, G. A. Parada, T.-C. Tang, E. Tham, C. de la Fuente-Nunez, T. K. Lu, X. Zhao, *Adv. Mater.* **2018**, *30*, 1704821.
[12] B. Chen, W. Kang, J. Sun, R. Zhu, Y. Yu, A. Xia, M. Yu, M. Wang, J. Han, Y. Chen, L. Teng, Q. Tian, Y. Yu, G. Li, L. You, Z. Liu, Z. Dai, *Nat. Chem. Biol.* **2022**, *18*, 289.
[13] C. Gilbert, T.-C. Tang, W. Ott, B. A. Dorr, W. M. Shaw, G. L. Sun, T. K. Lu, T. Ellis, *Nat. Mater.* **2021**, *20*, 691.
[14] X. Liu, T.-C. Tang, E. Tham, H. Yuk, S. Lin, T. K. Lu, X. Zhao, *Proc. Natl. Acad. Sci. USA* **2017**, *114*, 2200.
[15] F. Moser, E. Tham, L. M. González, T. K. Lu, C. A. Voigt, *Adv. Funct. Mater.* **2019**, *29*, 1901788.
[16] S. Sankaran, J. Becker, C. Wittmann, A. del Campo, *Small* **2019**, *15*, 1804717.
[17] T. G. Johnston, S.-F. Yuan, J. M. Wagner, X. Yi, A. Saha, P. Smith, A. Nelson, H. S. Alper, *Nat. Commun.* **2020**, *11*, 563.
[18] P. K. R. Tay, P. Q. Nguyen, N. S. Joshi, *ACS Synth. Biol.* **2017**, *6*, 1841.
[19] J. Pu, Y. Liu, J. Zhang, B. An, Y. Li, X. Wang, K. Din, C. Qin, K. Li, M. Cui, S. Liu, Y. Huang, Y. Wang, Y. Lv, J. Huang, Z. Cui, S. Zhao, C. Zhong, *Adv. Sci.* **2020**, *7*, 1903558.
[20] D. Datta, E. L. Weiss, D. Wangpraseurt, E. Hild, S. Chen, J. W. Golden, S. S. Golden, J. K. Pokorski, *Nat. Commun.* **2023**, *14*, 4742.
[21] C. M. Heveran, S. L. Williams, J. Qiu, J. Artier, M. H. Hubler, S. M. Cook, J. C. Cameron, W. V. Srubar, *Matter* **2020**, *2*, 481.
[22] R. M. McBee, M. Lucht, N. Mukhitov, M. Richardson, T. Srinivasan, D. Meng, H. Chen, A. Kaufman, M. Reitman, C. Munck, D. Schaak, C. Voigt, H. H. Wang, *Nat. Mater.* **2022**, *21*, 471.
[23] M. Lufton, O. Bustan, B.-h. Eylon, E. Shtifman-Segal, T. Croitoru-Sadger, A. Shagan, A. Shabtay-Orbach, E. Corem-Salkmon, J. Berman, A. Nyska, B. Mizrahi, *Adv. Funct. Mater.* **2018**, *28*, 1801581.
[24] P. Praveschotinunt, A. M. Duraj-Thatte, I. Gelfat, F. Bahl, D. B. Chou, N. S. Joshi, *Nat. Commun.* **2019**, *10*, 5580.
[25] A. M. Duraj-Thatte, N.-M. D. Courchesne, P. Praveschotinunt, J. Rutledge, Y. Lee, J. M. Karp, N. S. Joshi, *Adv. Mater.* **2019**, *31*, 1901826.
[26] L. M. González, N. Mukhitov, C. A. Voigt, *Nat. Chem. Biol.* **2020**, *16*, 126.
[27] J. Malda, J. Visser, F. P. Melchels, T. Jüngst, W. E. Hennink, W. J. A. Dhert, J. Groll, D. W. Hutmacher, *Adv. Mater.* **2013**, *25*, 5011.
[28] S. V. Murphy, A. Atala, *Nat. Biotech.* **2014**, *32*, 773.
[29] A. Skardal, A. Atala, *Ann. Biomed. Eng.* **2015**, *43*, 730.
[30] L. Moroni, J. A. Burdick, C. Highley, S. J. Lee, Y. Morimoto, S. Takeuchi, J. J. Yoo, *Nat. Rev. Mater.* **2018**, *3*, 21.
[31] J. Li, C. Wu, P. K. Chu, M. Gelinsky, *Mat. Sci. Eng. R Rep.* **2020**, *140*, 100543.
[32] R. Levato, T. Jungst, R. G. Scheuring, T. Blunk, J. Groll, J. Malda, *Adv. Mater.* **2020**, *32*, 1906423.
[33] Y. S. Zhang, G. Haghiashtiani, T. Hübscher, D. J. Kelly, J. M. Lee, M. Lutolf, M. C. McAlpine, W. Y. Yeong, M. Zenobi-Wong, J. Malda, *Nat. Rev. Methods Primers* **2021**, *1*, 75.
[34] S. M. Hull, L. G. Brunel, S. C. Heilshorn, *Adv. Mater.* **2022**, *34*, 2103691.
[35] J. K. Park, H. N. Chang, *Biotechnol. Adv.* **2000**, *18*, 303.
[36] P. Li, M. Müller, M. W. Chang, M. Frettlöh, H. Schönherr, *ACS Appl. Mater. Interfaces* **2017**, *9*, 22321.
[37] S. Guo, E. Dubuc, Y. Rave, M. Verhagen, S. A. E. Twisk, T. van der Hek, G. J. M. Oerlemans, M. C. M. van den Oetelaar, L. S. van Hazendonk, M. Brüls, B. V. Eijkens, P. L. Joostens, S. R. Keij, W. Xing, M. Nijs, J. Stalpers, M. Sharma, M. Gerth, R. J. E. A. Boonen, K. Verduin, M. Merkx, I. K. Voets, T. F. A. de Greef, *ACS Synth. Biol.* **2020**, *9*, 475.
[38] T.-C. Tang, E. Tham, X. Liu, K. Yehl, A. J. Rovner, H. Yuk, C. de la Fuente-Nunez, F. J. Isaacs, X. Zhao, T. K. Lu, *Nat. Chem. Biol.* **2021**, *17*, 724.
[39] L. Ouyang, J. P. K. Armstrong, Y. Lin, J. P. Wojciechowski, C. Lee-Reeves, D. Hachim, K. Zhou, J. A. Burdick, M. M. Stevens, *Sci. Adv.* **2020**, *6*, abc5529.
[40] H. Arslan, A. Davuluri, H. H. Nguyen, B. R. So, J. Lee, J. Jeon, K. Yum, *ACS Appl. Bio Mater.* **2024**, *7*, 7040.
[41] M. Schaffner, P. A. Rühs, F. Coulter, S. Kilcher, A. R. Studart, *Sci. Adv.* **2017**, *3*, aao6804.

[42] T. Billiet, E. Gevaert, T. De Schryver, M. Cornelissen, P. Dubruel, *Biomaterials* **2014**, *35*, 49.
[43] B. Webb, B. J. Doyle, *Bioprinting* **2017**, *8*, 8.
[44] B. A. Aguado, W. Mulyasasmita, J. Su, K. J. Lampe, S. C. Heilshorn, *Tissue Eng., Part A* **2011**, *18*, 806.
[45] A. Saha, T. G. Johnston, R. T. Shafranek, C. J. Goodman, J. G. Zalatan, D. W. Storti, M. A. Ganter, A. Nelson, *ACS Appl. Mater. Interfaces* **2018**, *10*, 13373.
[46] F. Qian, C. Zhu, J. M. Knipe, S. Ruelas, J. K. Stolaroff, J. R. DeOtte, E. B. Duoss, C. M. Spadaccini, C. A. Henard, M. T. Guarnieri, S. E. Baker, *Nano Lett.* **2019**, *19*, 5829.
[47] S. Gantenbein, E. Colucci, J. Käch, E. Trachsel, F. B. Coulter, P. A. Rühs, K. Masania, A. R. Studart, *Nat. Mater.* **2023**, *22*, 128.
[48] B. A. E. Lehner, D. T. Schmieden, A. S. Meyer, *ACS Synth. Biol.* **2017**, *6*, 1124.
[49] J. Huang, S. Liu, C. Zhang, X. Wang, J. Pu, F. Ba, S. Xue, H. Ye, T. Zhao, K. Li, Y. Wang, J. Zhang, L. Wang, C. Fan, T. K. Lu, C. Zhong, *Nat. Chem. Biol.* **2019**, *15*, 34.
[50] S. Balasubramanian, K. Yu, A. S. Meyer, E. Karana, M.-E. Aubin-Tam, *Adv. Funct. Mater.* **2021**, *31*, 2011162.
[51] A. M. Duraj-Thatte, A. Manjula-Basavanna, J. Rutledge, J. Xia, S. Hassan, A. Sourlis, A. G. Rubio, A. Lesha, M. Zenkl, A. Kan, D. A. Weitz, Y. S. Zhang, N. S. Joshi, *Nat. Commun.* **2021**, *12*, 6600.
[52] L. K. Rivera-Tarazona, T. Shukla, K. A. Singh, A. K. Gaharwar, Z. T. Campbell, T. H. Ware, *Adv. Funct. Mater.* **2022**, *32*, 2106843.
[53] S. Shin, H. Kwak, D. Shin, J. Hyun, *Nat. Commun.* **2019**, *10*, 4650.
[54] M. R. Binelli, P. A. Rühs, G. Pisaturo, S. Leu, E. Trachsel, A. R. Studart, *Biomater. Adv.* **2022**, *141*, 213095.
[55] T. J. Hinton, Q. Jallerat, R. N. Palchesko, J. H. Park, M. S. Grodzicki, H.-J. Shue, M. H. Ramadan, A. R. Hudson, A. W. Feinberg, *Sci. Adv.* **2015**, 1.
[56] C. B. Highley, C. B. Rodell, J. A. Burdick, *Adv. Mater.* **2015**, *27*, 5075.
[57] T. Bhattacharjee, S. M. Zehnder, K. G. Rowe, S. Jain, R. M. Nixon, W. G. Sawyer, T. E. Angelini, *Sci. Adv.* **2015**, *1*, 1500655.
[58] A. Lee, A. R. Hudson, D. J. Shiwarski, J. W. Tashman, T. J. Hinton, S. Yerneni, J. M. Bliley, P. G. Campbell, A. W. Feinberg, *Science* **2019**, *365*, 482.
[59] A. McCormack, C. B. Highley, N. R. Leslie, F. P. W. Melchels, *Trends Biotechnol.* **2020**, *38*, 584.
[60] D. J. Shiwarski, A. R. Hudson, J. W. Tashman, A. W. Feinberg, *APL Bioeng.* **2021**, 5.
[61] W. Wu, A. DeConinck, J. A. Lewis, *Adv. Mater.* **2011**, *23*, H178.
[62] J. S. Miller, K. R. Stevens, M. T. Yang, B. M. Baker, D.-H. T. Nguyen, D. M. Cohen, E. Toro, A. A. Chen, P. A. Galie, X. Yu, R. Chaturvedi, S. N. Bhatia, C. S. Chen, *Nat. Mater.* **2012**, *11*, 768.
[63] D. B. Kolesky, R. L. Truby, A. S. Gladman, T. A. Busbee, K. A. Homan, J. A. Lewis, *Adv. Mater.* **2014**, *26*, 3124.
[64] D. B. Kolesky, K. A. Homan, M. A. Skylar-Scott, J. A. Lewis, *Proc. Natl. Acad. Sci. USA* **2016**, *113*, 3179.
[65] X. Ma, X. Qu, W. Zhu, Y.-S. Li, S. Yuan, H. Zhang, J. Liu, P. Wang, C. S. E. Lai, F. Zanella, G.-S. Feng, F. Sheikh, S. Chien, S. Chen, *Proc. Natl. Acad. Sci. USA* **2016**, *113*, 2206.
[66] S. H. Kim, Y. K. Yeon, J. M. Lee, J. R. Chao, Y. J. Lee, Y. B. Seo, M. T. Sultan, O. J. Lee, J. S. Lee, S.-I. Yoon, I.-S. Hong, G. Khang, S. J. Lee, J. J. Yoo, C. H. Park, *Nat. Commun.* **2018**, *9*, 1620.
[67] K. Dubbin, Z. Dong, D. M. Park, J. Alvarado, J. Su, E. Wasson, C. Robertson, J. Jackson, A. Bose, M. L. Moya, Y. Jiao, W. F. Hynes, *Nano Lett.* **2021**, *21*, 1352.
[68] G. Altin-Yavuzarslan, S. M. Brooks, S.-F. Yuan, J. O. Park, H. S. Alper, A. Nelson, *Adv. Funct. Mater.* **2023**, *33*, 2300332.
[69] G. Altin-Yavuzarslan, N. Sadaba, S. M. Brooks, H. S. Alper, A. Nelson, *Small* **2024**, *20*, 2306564.
[70] F. P. W. Melchels, J. Feijen, D. W. Grijpma, *Biomaterials* **2010**, *31*, 6121.
[71] J. A. S. Neiman, R. Raman, V. Chan, M. G. Rhoads, M. S. B. Raredon, J. J. Velazquez, R. L. Dyer, R. Bashir, P. T. Hammond, L. G. Griffith, *Biotechnol. Bioeng.* **2015**, *112*, 777.
[72] B. H. Cumpston, S. P. Ananthavel, S. Barlow, D. L. Dyer, J. E. Ehrlich, L. L. Erskine, A. A. Heikal, S. M. Kuebler, I. Y. S. Lee, D. McCord-Maughon, J. Qin, H. Röckel, M. Rumi, X.-L. Wu, S. R. Marder, J. W. Perry, *Nature* **1999**, *398*, 51.
[73] W. Zhang, P. Soman, K. Meggs, X. Qu, S. Chen, *Adv. Funct. Mater.* **2013**, *23*, 3226.
[74] J. L. Connell, E. T. Ritschdorff, M. Whiteley, J. B. Shear, *Proc. Natl. Acad. Sci. USA* **2013**, *110*, 18380.
[75] R. Gaebel, N. Ma, J. Liu, J. Guan, L. Koch, C. Klopsch, M. Gruene, A. Toelk, W. Wang, P. Mark, F. Wang, B. Chichkov, W. Li, G. Steinhoff, *Biomaterials* **2011**, *32*, 9218.
[76] L. Koch, A. Deiwick, S. Schlie, S. Michael, M. Gruene, V. Coger, D. Zychlinski, A. Schambach, K. Reimers, P. M. Vogt, B. Chichkov, *Biotechnol. Bioeng.* **2012**, *109*, 1855.
[77] P. Serra, A. Piqué, *Adv. Mater. Technol.* **2019**, *4*, 1800099.
[78] W. Zhu, X. Ma, M. Gou, D. Mei, K. Zhang, S. Chen, *Curr. Opin. Biotechnol.* **2016**, *40*, 103.
[79] V. S. Cheptsov, E. S. Churbanova, V. I. Yusupov, M. V. Gorlenko, L. V. Lysak, N. V. Minaev, V. N. Bagratashvili, B. N. Chichkov, *Lett. Appl. Microbiol.* **2018**, *67*, 544.
[80] B. E. Kelly, I. Bhattacharya, H. Heidari, M. Shusteff, C. M. Spadaccini, H. K. Taylor, *Science* **2019**, *363*, 1075.
[81] J. T. Toombs, M. Luitz, C. C. Cook, S. Jenne, C. C. Li, B. E. Rapp, F. Kotz-Helmer, H. K. Taylor, *Science* **2022**, *376*, 308.
[82] P. N. Bernal, P. Delrot, D. Loterie, Y. Li, J. Malda, C. Moser, R. Levato, *Adv. Mater.* **2019**, *31*, 1904209.
[83] P. N. Bernal, M. Bouwmeester, J. Madrid-Wolff, M. Falandt, S. Florczak, N. G. Rodriguez, Y. Li, G. Größbacher, R.-A. Samsom, M. van Wolferen, L. J. W. van der Laan, P. Delrot, D. Loterie, J. Malda, C. Moser, B. Spee, R. Levato, *Adv. Mater.* **2022**, *34*, 2110054.
[84] M. Xie, L. Lian, X. Mu, Z. Luo, C. E. Garciamendez-Mijares, Z. Zhang, A. López, J. Manríquez, X. Kuang, J. Wu, J. K. Sahoo, F. Z. González, G. Li, G. Tang, S. Maharjan, J. Guo, D. L. Kaplan, Y. S. Zhang, *Nat. Commun.* **2023**, *14*, 210.
[85] W. Qiu, J. Gehlen, M. Bernero, C. Gehre, G. N. Schädli, R. Müller, X.-H. Qin, *Adv. Funct. Mater.* **2023**, *33*, 2214393.
[86] D. Ribezzi, M. Gueye, S. Florczak, F. Dusi, D. de Vos, F. Manente, A. Hierholzer, M. Fussenegger, M. Caiazzo, T. Blunk, J. Malda, R. Levato, *Adv. Mater.* **2023**, *35*, 2301673.
[87] M. B. Riffe, M. D. Davidson, G. Seymour, A. P. Dhand, M. E. Cooke, H. M. Zlotnick, R. R. McLeod, J. A. Burdick, *Adv. Mater. 36*, 2309026.
[88] B. Pabst, B. Pitts, E. Lauchnor, P. S. Stewart, *Antimicrob. Agents Chemother.* **2016**, *60*, 6294.
[89] K. A. Moore, S. Altus, J. W. Tay, J. B. Meehl, E. B. Johnson, D. M. Bortz, J. C. Cameron, *Nat. Microbiol.* **2020**, *5*, 757.
[90] H. Priks, T. Butelmann, A. Illarionov, T. G. Johnston, C. Fellin, T. Tamm, A. Nelson, R. Kumar, P.-J. Lahtvee, *ACS Appl. Bio Mater.* **2020**, *3*, 4273.
[91] S. Bhusari, S. Sankaran, A. del Campo, *Adv. Sci.* **2022**, *9*, 2106026.
[92] P. S. Stewart, M. J. Franklin, *Nat. Rev. Microbiol.* **2008**, *6*, 199.
[93] H.-C. Flemming, J. Wingender, *Nat. Rev. Microbiol.* **2010**, *8*, 623.
[94] H.-C. Flemming, J. Wingender, U. Szewzyk, P. Steinberg, S. A. Rice, S. Kjelleberg, *Nat. Rev. Microbiol.* **2016**, *14*, 563.
[95] J. Lee, S. J. Oh, S. H. An, W.-D. Kim, S.-H. Kim, *Biofabrication* **2020**, *12*, 035018.
[96] J. Kerner, A. Dogan, H. von Recum, *Acta Biomater.* **2021**, *130*, 54.
[97] A. Suwardi, F. Wang, K. Xue, M.-Y. Han, P. Teo, P. Wang, S. Wang, Y. Liu, E. Ye, Z. Li, X. J. Loh, *Adv. Mater.* **2022**, *34*, 2102703.

[98] S. M. McDonald, E. K. Augustine, Q. Lanners, C. Rudin, L. C Brinson, M. L. Becker, *Nat. Commun.* **2023**, *14*, 4838.
[99] Y. Mei, K. Saha, S. R. Bogatyrev, J. Yang, A. L. Hook, Z. I. Kalcioglu, S.-W. Cho, M. Mitalipova, N. Pyzocha, F. Rojas, K. J. Van Vliet, M. C. Davies, M. R. Alexander, R. Langer, R. Jaenisch, D. G. Anderson, *Nat. Mater.* **2010**, *9*, 768.
[100] A. L. Hook, D. G. Anderson, R. Langer, P. Williams, M. C. Davies, M. R. Alexander, *Biomaterials* **2010**, *31*, 187.
[101] M. A. Alcantar, M. A. English, J. A. Valeri, J. J. Collins, *Mol. Cell* **2024**, *84*, 2382.
[102] A. Y. Chen, Z. Deng, A. N. Billings, U. O. S. Seker, M. Y. Lu, R. J. Citorik, B. Zakeri, T. K. Lu, *Nat. Mater.* **2014**, *13*, 515.
[103] P. Q. Nguyen, Z. Botyanszki, P. K. R. Tay, N. S. Joshi, *Nat. Commun.* **2014**, *5*, 4945.
[104] S. Tibbits, *Archit. Des.* **2014**, *84*, 116.
[105] A. S. Gladman, E. A. Matsumoto, R. G. Nuzzo, L. Mahadevan, J. A. Lewis, *Nat. Mater.* **2016**, *15*, 413.
[106] H. Arslan, A. Nojoomi, J. Jeon, K. Yum, *Adv. Sci.* **2019**, *6*, 1800703.
[107] J. Kim, J. A. Hanna, M. Byun, C. D. Santangelo, R. C. Hayward, *Science* **2012**, *335*, 1201.
[108] A. Nojoomi, H. Arslan, K. Lee, K. Yum, *Nat. Commun.* **2018**, *9*, 3705.
[109] A. Nojoomi, J. Jeon, K. Yum, *Nat. Commun.* **2021**, *12*, 603.
[110] L. K. Rivera-Tarazona, V. D. Bhat, H. Kim, Z. T. Campbell, T. H. Ware, *Sci. Adv.* **2020**, *6*, aax8582.
[111] L. K. Rivera-Tarazona, Z. T. Campbell, T. H. Ware, *Soft Matter* **2021**, *17*, 785.
[112] A. W. Feinberg, A. Feigel, S. S. Shevkoplyas, S. Sheehy, G. M. Whitesides, K. K. Parker, *Science* **2007**, *317*, 1366.
[113] K. Kuribayashi-Shigetomi, H. Onoe, S. Takeuchi, *PLoS One* **2012**, *7*, 51085.
[114] J. C. Nawroth, H. Lee, A. W. Feinberg, C. M. Ripplinger, M. L. McCain, A. Grosberg, J. O. Dabiri, K. K. Parker, *Nat. Biotechnol.* **2012**, *30*, 792.
[115] R. Raman, C. Cvetkovic, S. G. M. Uzel, R. J. Platt, P. Sengupta, R. D. Kamm, R. Bashir, *Proc. Natl. Acad. Sci. USA* **2016**, *113*, 3497.
[116] S.-J. Park, M. Gazzola, K. S. Park, S. Park, V. Di Santo, E. L. Blevins, J. U. Lind, P. H. Campbell, S. Dauth, A. K. Capulli, F. S. Pasqualini, S. Ahn, A. Cho, H. Yuan, B. M. Maoz, R. Vijaykumar, J.-W. Choi, K. Deisseroth, G. V. Lauder, L. Mahadevan, K. K. Parker, *Science* **2016**, *353*, 158.
[117] A. G. Rottinghaus, A. Ferreiro, S. R. S. Fishbein, G. Dantas, T. S. Moon, *Nat. Commun.* **2022**, *13*, 672.
[118] Y. Ma, A. Manna, T. S. Moon, *Curr. Opin. Syst. Biol.* **2023**, *36*, 100483.
[119] A. M. Hartig, W. Dai, K. Zhang, K. Kapoor, A. G. Rottinghaus, T. S. Moon, K. M. Parker, *Environ. Sci. Technol.* **2024**, *58*, 22657.
[120] T. S. Moon, *New Biotechnol.* **2023**, *78*, 150.

Tae Seok Moon is a YouTuber, director of an NSF global center, professor at JCVI, EBRC Council Member, SynBYSS Chair, Moonshot Bio founder, EFB Executive Board Member, and editor of 10 journals, including the New Biotechnology Editor-in-Chief. He has expertise in Systems and Synthetic Biology. He aims to solve global agricultural, environmental, manufacturing, and health problems through engineering biology. His service to SynBYSS provides a weekly forum for more than 1000 global audiences. The 417 speakers include a Nobel Laureate, 24 National Academy Members, 42 funders, 20 Editors-in-chief, 11 Nature/Cell journal editors, and 199 rising stars.

Kyungsuk Yum is an associate professor in the Department of Materials Science and Engineering at the University of Texas at Arlington. He earned his Ph.D. in mechanical engineering from the University of Illinois at Urbana-Champaign. He subsequently worked as a postdoctoral research associate in chemical engineering at MIT and bioengineering at the University of California, Berkeley. His research interests include bioinspired materials and engineering, soft materials, and 3D/4D printing.